Final Report: Reducing Whole-Body Vibrations in Neonatal Transport

December 14th, 2022

BME 300/200

Clients: Dr. Ryan McAdams and Dr. Joshua Gollub

Advisor: Dr. Justin Williams

Team Members:

Team Leader: Joshua Varghese

Communicator: Sydney Therien

BWIG: Neha Kulkarni

BWIG: Julia Salita

BPAG: Joey Byrne

BSAC: Greta Scheidt

Abstract

Transport puts extreme stress on neonates, who are often in critical condition, lowering their chance of survival [1]. Vibrational forces experienced by neonates during transport have been linked to an increased odds of severe brain injury. In particular, intraventricular hemorrhaging (IVH) can lead to neurodevelopmental impairment or death [2], [3]. However, there is no standardized device to mitigate vibrational forces. To resolve this issue, a metal and gel composite damper has been proposed to help mitigate the harsh vibrations. The damper consists of four layers: silicone gel, aluminum, foam, and stainless steel. This design was inspired by the anatomy of a woodpecker, which can naturally reduce the vibrations that its head experiences during pecking. A total of four dampers were placed between the inner and outer trays of the transport isolette. Two configurations of dampers were produced: one to be inserted along the side of the inner tray and one to be inserted in the front corners of the tray. Accelerometer and gyroscope data were collected from various locations in the ambulance with and without the dampers during a test route to quantify the effect of the dampers on the magnitude and direction of vibrations. Results from testing showed that the damper was not effective in reducing the average acceleration inside the incubator to be below the target threshold of 0.87 m/s^2 [4]. However, further analysis of the results showed that there was a significant reduction in vibrations compared to the incubator setup without the prototype implemented.

Table of Contents

I. Introduction

Motivation

The quality of transport for critically-ill neonates to a Neonatal Intensive Care Unit (NICU) directly influences chances of survival or morbidity [5]. The critically-ill neonate is often the result of a preterm birth (< 37 complete weeks of gestation) or underlying birth defects [6]. One in ten neonates need access to a NICU in the first week of life [7]. 1.3% of neonates are born *ex-utero* and must be transported to a NICU via ambulance or helicopter [8]. The current methods of transport expose a neonate to whole-body vibrations (WBV), translational and rotational motion, and excessive sound [4]. The effects of *ex-utero* transfer are well-documented in studies which conclude that transportation of a neonate significantly increases the odds of severe brain injury (odds ratio of 2.32) and significantly lowers the odds of survival without brain injury (odds ratio of 0.60) [2], [3]. One brain injury of concern is intraventricular hemorrhaging (IVH), which is closely associated with neonatal transport and can lead to subsequent neurodevelopmental impairment or death [9]. Therefore, reducing vibrations, mechanical forces, and excessive sound has the potential to significantly improve the outcomes of neonatal transport. There is no standardized vibration-reducing device used in neonatal transport, reflecting the need for a device that minimizes the environmental stressors transferred through the transport vehicle.

Existing Devices and Current Methods

The current methods of minimizing vibrations and mechanical forces by the UW Hospital's neonatal transport teams involve the use of a Geo-Matrix mattress, a five-point harness, various pillows, and suspension systems. The gel mattress in the incubator is placed directly under the neonate during transport. The five-point harness secures the neonate in place using straps across the shoulders, hips, and thighs [10]. The transport team uses additional pillows and blankets to manipulate the position of the neonate or support the head. The transport vehicle's suspension system as well as the built-in suspension system on the gurney act to reduce forces exerted by the ground.

These methods are insufficient in reducing vibrations and mechanical forces felt by the neonate, as whole-body vibration levels often exceed the recommended 0.87 m/s^2 in adults [4]. No standards have been developed for the recommended maximum vibration levels for neonates, but it can be reasonably assumed that it is significantly less than the level for fully-developed adults. The current method does very little to mitigate vibrations and features many rigid parts directly in contact with one another.

The current method for minimizing excessive sound by the UW Medflight team is using a pair of ear muffs that are placed over the neonate's ears during transport. While effective at minimizing sound, the ear muffs used are easily displaced by movement of the vehicle or neonate. Thus, this is an ineffective method for mitigating excessive sound levels as the medical transport team does not have easy access to constantly adjust the ear muffs.

While no vibration-reducing device has been established as a standard for neonatal transport, several products have been created for this purpose. The first is the Quasi-Zero-Stiffness (QZS) Isolator (a1, Fig. 1) which identifies and targets low-frequency components as the primary disturbing vibration [11]. This product modifies the incubator control box (a3, Fig. 1), located directly below the incubator (a2, Fig. 1) by adding four QZS Isolators in each corner of the housing. Each QZS Isolator has a pair of repelling ring permanent magnets (c4 & c5, Fig. 1) that are connected in parallel to a coil spring (c9, Fig. 1). The inner ring magnet (c4, Fig. 1) is fixed to a central rod (c1, Fig. 1), while the outer ring magnet (c5, Fig. 1) is fixed on the sleeve (c7, Fig. 1) that surrounds the rod. The concentric system of ring magnets mitigates the effects of rotational and translational motion and keeps the isolators aligned vertically, allowing the coil spring (c9, Fig. 1) to take on most of the weight. Finally, a viscous damper (c10, Fig. 1) is added inside the coil spring (c9, Fig. 1) to help reduce vibrations and forces in the vertical direction. Although the concept of QZS Isolators is well supported, the design involves substantial alterations to the current transport setup, has a complicated design, and lacks experimental testing to verify its ability to reduce whole body vibrations.

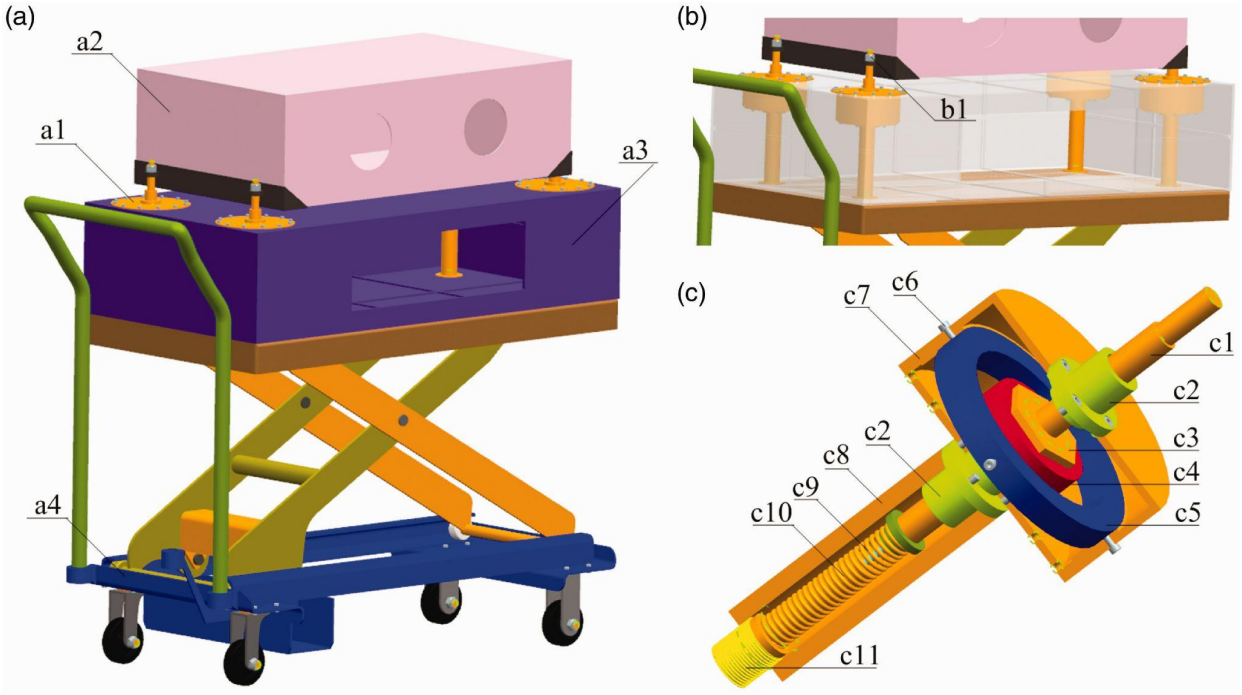

Figure 1: (a) an overview of the QZS vibration isolation system; (b) the installation view of the QZS isolators into the incubator control box; (c) the inside view of the QZS isolator [11].

A second design, referred to as an isolation device for shock reduction occupies the space between the isolette and the stretcher platform, and can be seen in Figure 2 [12]. The design features pairs of metal plates that serve as attachment points for gas or air springs. One plate is mounted to the top of the gurney while the other plate is mounted to the bottom of the isolette. Air or gas springs are fixed between the plates in order to provide dampening effects for the isolette. The pressure within the air springs can be adjusted to attenuate high or low frequencies of vibration. The design specifies that two air springs are placed in each corner and one is placed in the center. A patent application has been submitted for the use of parallel plates and air springs to reduce the transmission of kinetic energy between an isolette and support table (Application Number 11/540743). Similarly to the QZS Isolators, this design involves large modifications to the current transport setup. Additionally, it neglects the presence of the monitoring systems and

associated housing which are located directly below the isolette.

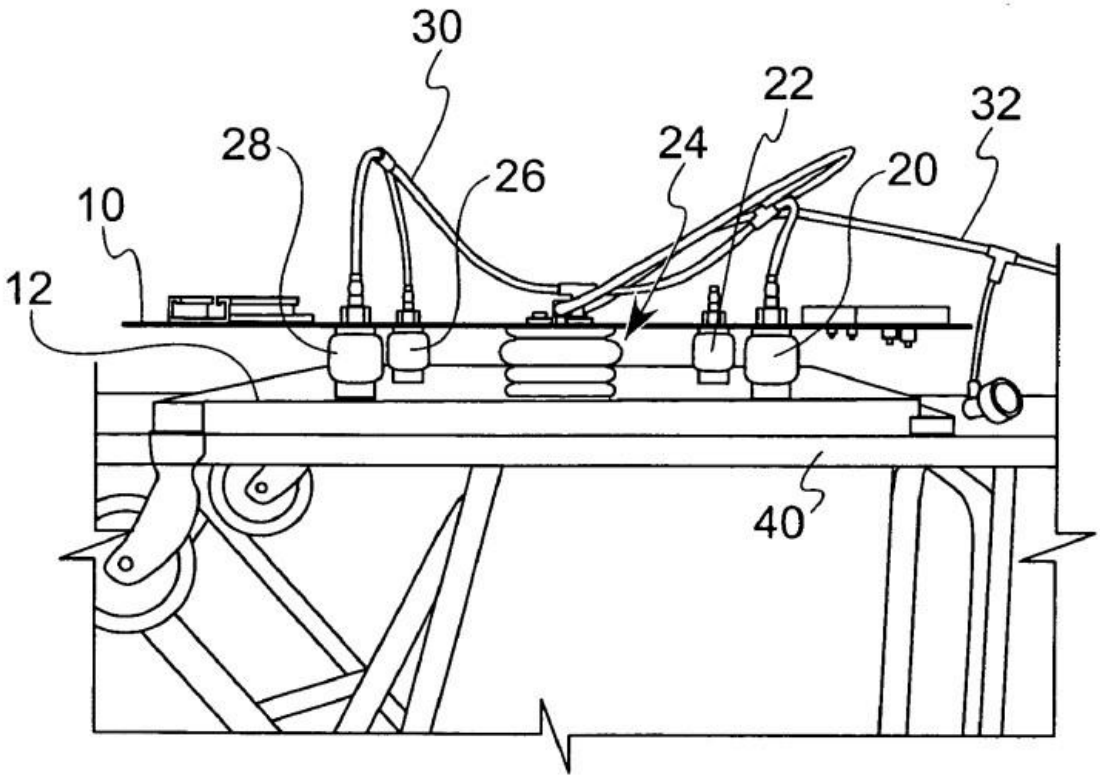

Figure 2: A side view of the isolation device for shock reduction in an operable position on the stretcher platform [12].

Problem Statement

Whole-body vibrations, translational forces, rotational moments, and excessive sound from a medical transport vehicle can cause brain injuries to critically-ill neonates that lead to neurodevelopmental impairment or death. Mitigating these physiological stressors has the potential to drastically improve transport outcomes including increased survival rates and decreased brain injury. The current transport setup neglects the effects of the stressors aforementioned by including a collection of rigid parts and only a single mattress to dampen vibrations. Thus, the client has tasked the team with developing a vibration-reducing device with mitigating mechanical forces and sound as secondary foci. The device must reduce each physiological stressor, so the neonate does not sustain injury, must fit within the dimensions of a standard ambulance and helicopter without interfering with the movement of the transport team,

and must be compatible with current incubator setup or include all the associated functions and equipment (**Appendix A**).

II. **Background**

Relevant Physiology and Biology

The neonate brain is highly susceptible to injury due to its underdeveloped nature and lack of structural support systems. A neonate's brain is very soft (often compared to unset gelatin) and as a result very vulnerable [13]. Within the brain, neuronal-glial precursor cells make up a vascularized region called the germinal matrix [14]. This region is particularly vulnerable for infants due to weaknesses in the blood-brain barrier in the first 48 hours of life. Moreover, premature infants struggle with cerebral autoregulation, which is the ability of cerebral vessels to keep constant cerebral blood flow (CBF) regardless of changes in arterial blood pressure. The smooth muscle cells and pericytes responsible for minimizing variations of CBF are not fully developed. A fluctuating CBF is associated with pressure passivity in regards to cerebral circulation. Additionally, the neonate's central nervous system is at a very immature stage and is constantly undergoing organizational changes [15]. These changes, combined with physiological instability, limit a neonate's ability to coordinate autonomic and self-regulatory responses towards environmental stressors.

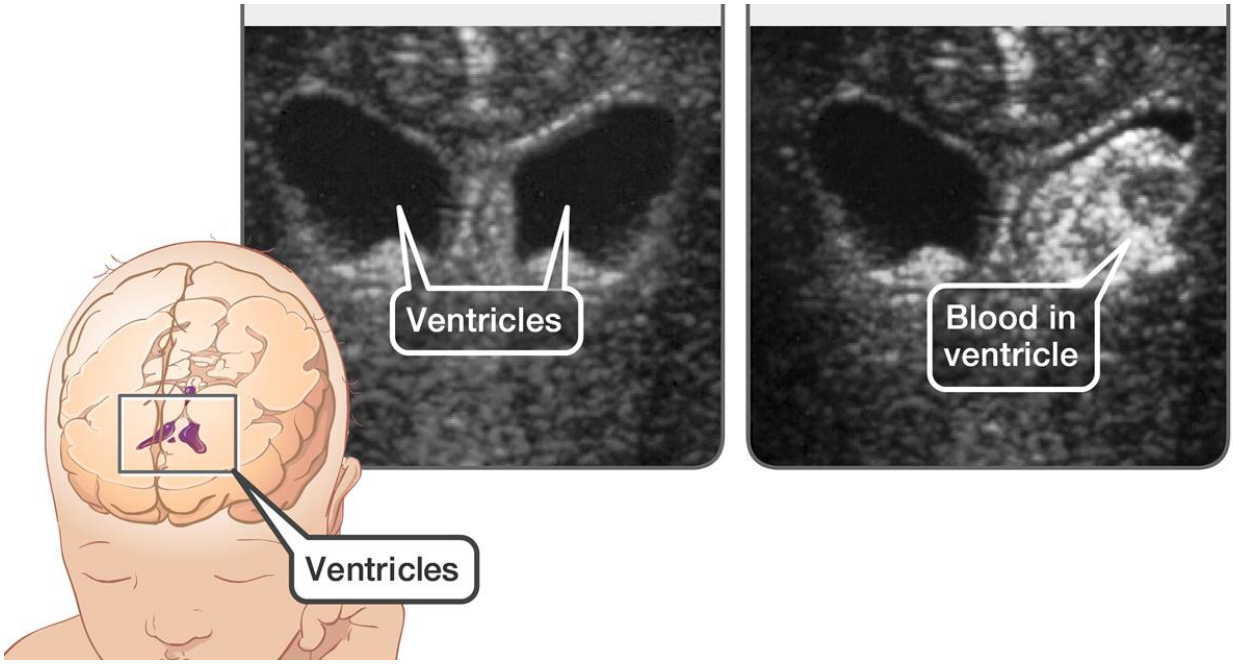

Figure 3: Healthy and IVH CT scans of the neonate ventricles with an anatomical reference on the left [16].

The fragility of a neonate brain described above increases susceptibility to intraventricular hemorrhage (IVH). The capillaries of the highly vascular germinal matrix are especially vulnerable to rupture when the neonate experiences whole-body vibrations [14]. Whole body vibrations can trigger IVH through a cumulative process beginning with cerebral vasoconstriction, increased free radicals, decreased nitric oxide, decreased cerebral blood flow, and repeated reperfusion injury [4]. These characteristics describe the progression of germinal matrix hemorrhage [14], as shown in Figure 3. Furthermore, there is a proven link between fluctuating cerebral blood flow velocity, commonly found in premature neonates, and higher chances of IVH. The nature of ground or air transport in conjunction with the neonate's unstable condition reveals the susceptibility of neonates to brain injury.

Relevant Design Information

The prospective design must function in conjunction with the preexisting setup. Understanding the organization of the transport setup is crucial to understanding design ideas and constraints. Descriptions of the setup are based on observations made from the transport incubator at UW Health, which is International Biomedical's Voyager model [17]. Regardless of

the model, all transport incubators follow the same general structure. The setup includes an incubator (also known as an isolette) which encloses the neonate during transport. A removeable, inner tray supports a mattress and fixes on to a permanent, outer tray on the bottom of the incubator. Below the incubator is metal housing for the incubator's control systems in order to regulate the environment of the incubator (e.g. temperature). This housing, with the incubator latched on top of it, is latched to a transport platform (also known as the deck). Also attached to the deck are a variety of support systems (e.g. oxygen tanks). The deck is then secured onto the gurney for transport.

Also consulted for guidance in developing a device to help reduce vibrations in neonatal transport was Dr. Heidi Kamrath, the transport director for Children's Hospitals and Clinics of Minnesota. Dr. Kamrath provided the team with insight into common issues faced during transportation of neonates and gave the team some objectives to aim for in the design of such a device. She emphasized that any such device must not impede the ability of the medical professionals to administer care. She told the team that an ideal device would, if everything was to go awry during a transport, have minimal ability to create more issues. The conversation with Dr. Kamrath informed many of the requirements outlined in the Product Design Specifications (**Appendix A**).

Client Information

Dr. Ryan McAdams is the Neonatology Division Chief for UW Health and a professor for the UW School of Medicine and Public Health. Dr. Joshua Gollub is a fellow at the University of Wisconsin School of Medicine and Public Health specializing in neonatal medicine.

Design Specifications

The client has tasked the team with developing a device to reduce whole-body vibrations which can cause stress to a neonate during transport in an ambulance. The client requires that the device satisfy several identified problems, which guided the requirements for the project as elaborated in the Product Design Specifications (**Appendix A**). The device must minimize vibrational forces below 0.87 m/s^2 for the entire duration of the transport [4]. The device must mitigate the effects of translational and rotational motion so that the neonate does not sustain

injury. A sound-reducing feature must be added to the device to reduce sound levels below the maximum accepted level of 45 dB [18]. The device must attach to the current incubators or include all the associated functions and equipment. Finally, the device must fit within the dimensions of a standard ambulance while allowing efficient movement of the transport team. Due to the constant nature of vibrations and motion during transport, the design should provide continuous functionality without disrupting the support systems and monitoring equipment. In terms of ergonomics, the device should be relatively easy to install and remove and require no additional manipulation once installed. The goal was to create a pilot model (i.e. functional prototype) that can be tested in mock ambulance transports and be implemented as part of the standard transport equipment.

III. Preliminary Designs

The team brainstormed several solutions to address the problem of reducing whole body vibrations to provide neonates with an improved chance of survival. The team decided on three designs to be formally illustrated and evaluated, each with distinct properties and methods to reduce vibrations.

Magnet-Induced Levitation Device

The first of these designs utilized the repulsion force created by magnets when two ends of the same polarity are in close proximity. The goal of this device was to create a combination of attractive and repulsive forces beneath the incubator that would act as a cushion and absorb any vibrations encountered during transport. As such, it was named the Magnet-Induced Levitation Device.

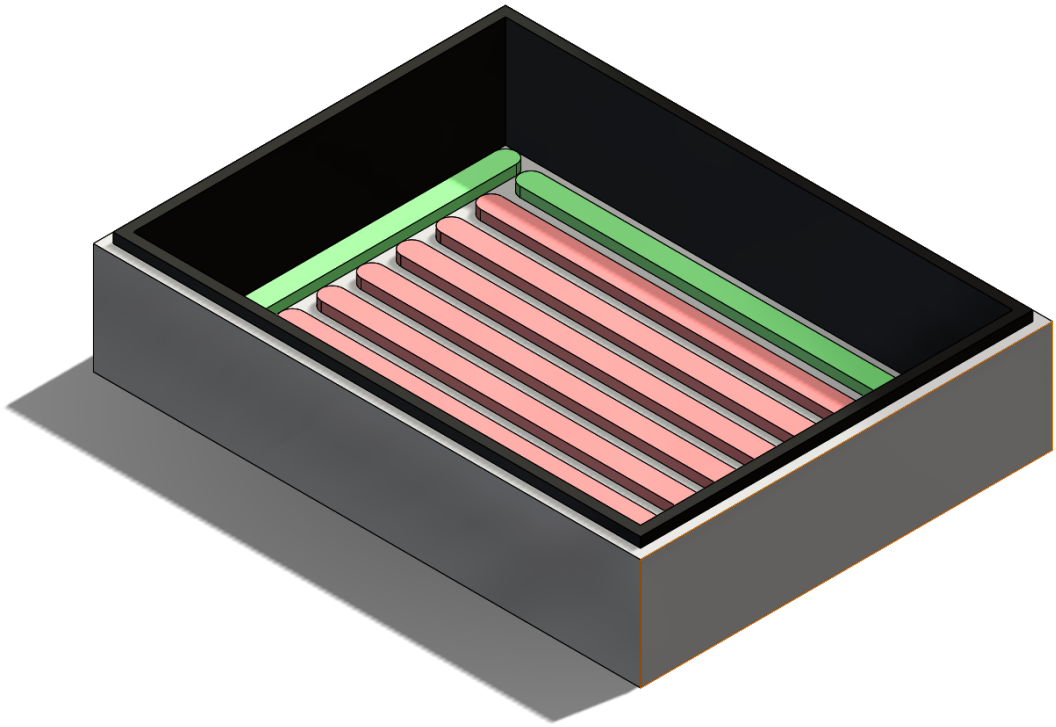

Figure 4: A SolidWorks sketch of the Magnet-Induced Levitation Device. Red magnets denote a repulsive force while green magnets represent an attractive force. The raised black interior is the foam layer that surrounds the horizontal translation prevention track.

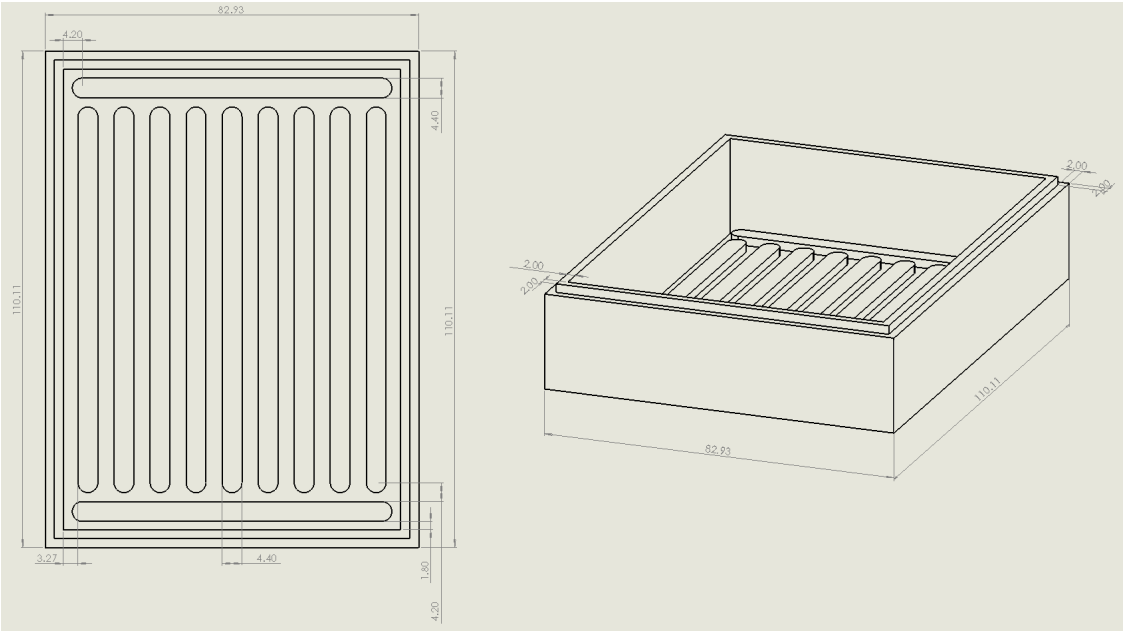

Figure 5: A SolidWorks drawing of the Magnet-Induced Levitation Design. The left side shows a top view and the right shows a dimetric side view. All dimensions are in cm.

As can be seen in Figure 5, the device utilizes strips of magnets of both polarities, with repelling forces (denoted with red in Fig. 4) in the center and attracting forces (denoted with green in Fig. 4**)** along the edges. The repelling magnets create the cushion while the attracting magnets stabilize the device and ensure that if the ambulance encounters any large bumps (railroad tracks, for example), the incubator will not be excessively displaced vertically. Horizontal translation of the incubator is inhibited by the placement of a foam-coated track around the sides of the incubator. The 2 cm thick foam layer would ideally eliminate vibrations produced by slight horizontal displacement.

Metal and Gel Composite Damper

The second design considered was a damper consisting of metal and gel concentric layers. The goal of the damper design was to reduce the magnitude of high-frequency vibrational forces that are exerted on the neonate during transport by dissipating forces applied to the tray inside the isolette and employing materials that could act as low-frequency mechanical filters. The design is L-shaped and would attach to the corners of the incubator's inner tray with ball-and-socket joints, as shown in Figure 6. The joints will convert the incubator's vibration of the inner tray into a gentle rocking motion. A close-up view of this joint system can be seen in Figure 7**.**

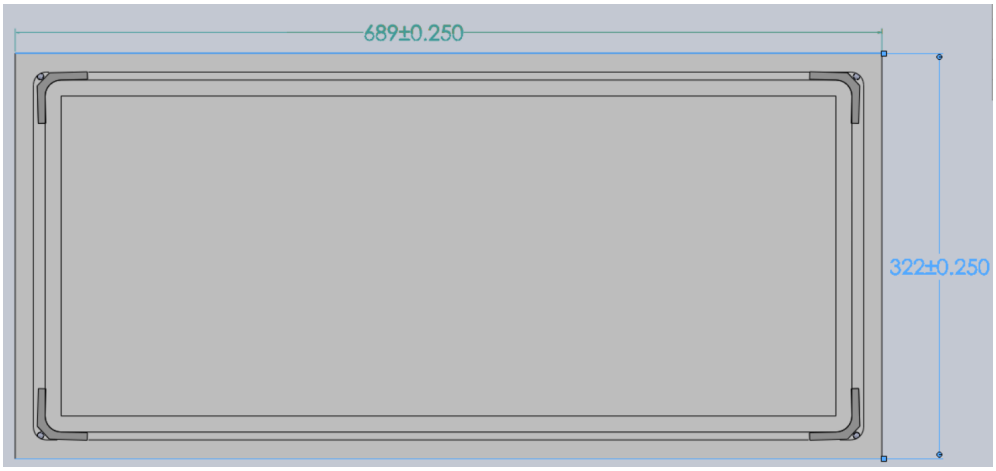

Figure 6: A SolidWorks sketch of the Metal and Gel Composite Damper from the top plane. All dimensions are in mm.

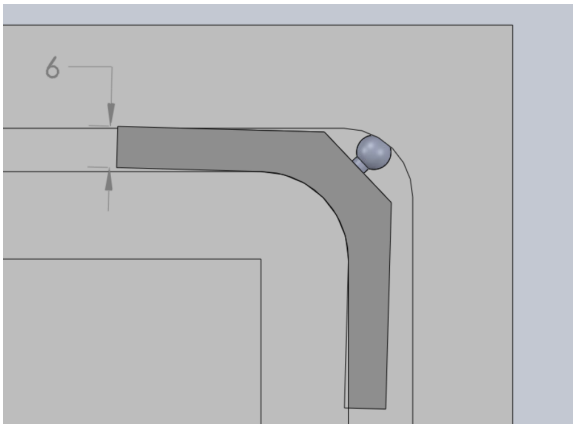

Figure 7: A close-up view of the ball-and-socket joint that connects the damper system to the outer tray of the incubator. All dimensions are in mm.

The damper consists of four layers of different materials which were chosen based upon their ability to mimic the unique and natural vibration-reduction properties of a woodpecker's head structure as shown in Figure 8 [19]. Through a system which can be divided into four features, woodpeckers are able to prevent most of the vibrational forces exerted on their beaks during pecking from reaching the brain.

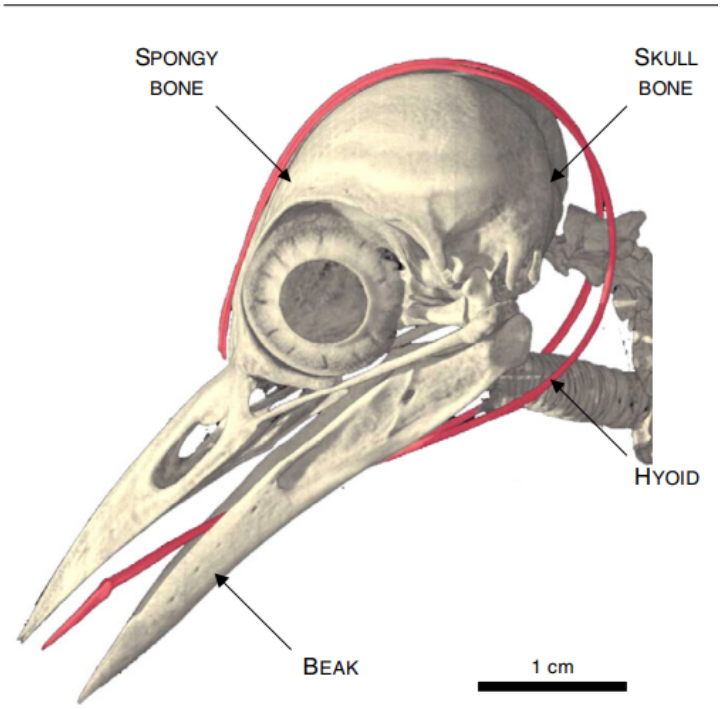

Figure 8: Four key vibration-reducing features of the woodpecker head structure are shown: the beak, the hyoid, skull bone, and spongy bone [20].

The head structure components of the beak, the hyoid which provides structure to the tongue, the skull bone with cerebrospinal fluid, and the spongy bone were correlated to man-made materials in the work of Biju et. al (Table 1), who utilized the natural vibration reduction properties of woodpecker anatomy to construct and test shock-absorbing structures.

Table 1: The materials that were correlated to anatomical features of the woodpecker are shown below [19].

Woodpecker	**Layered shock absorbing structure**
Beak	Metal (steel) enclosure I
Hyoid	Viscoelastic layer (foam)
Spongy bone	Metallic Beads
Skull bone with CSF	Metal (aluminium) enclosure II

This experimental study formed the basis of the metal/gel composite damper design. The materials chosen for the preliminary design had similar material properties to those shown in Table 1 and can be visualized in Figure 9. The innermost is a silicone gel, which is wrapped in a thin layer of aluminum. The third layer is a thicker coating of foam, which is encased in a thin layer of stainless steel, forming a medical-grade exterior that is easy to sterilize.

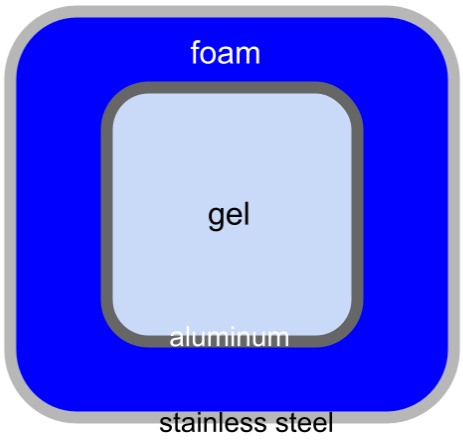

Figure 9: A labeled cross-sectional view of the concentric four-layered damper system.

Dampening curves from Biju et. al showed promising results for vibration reduction of this composite material, which can be seen in Figure 10 [19]. Application of this damper for vibrations in an incubator has the potential to be immensely successful.

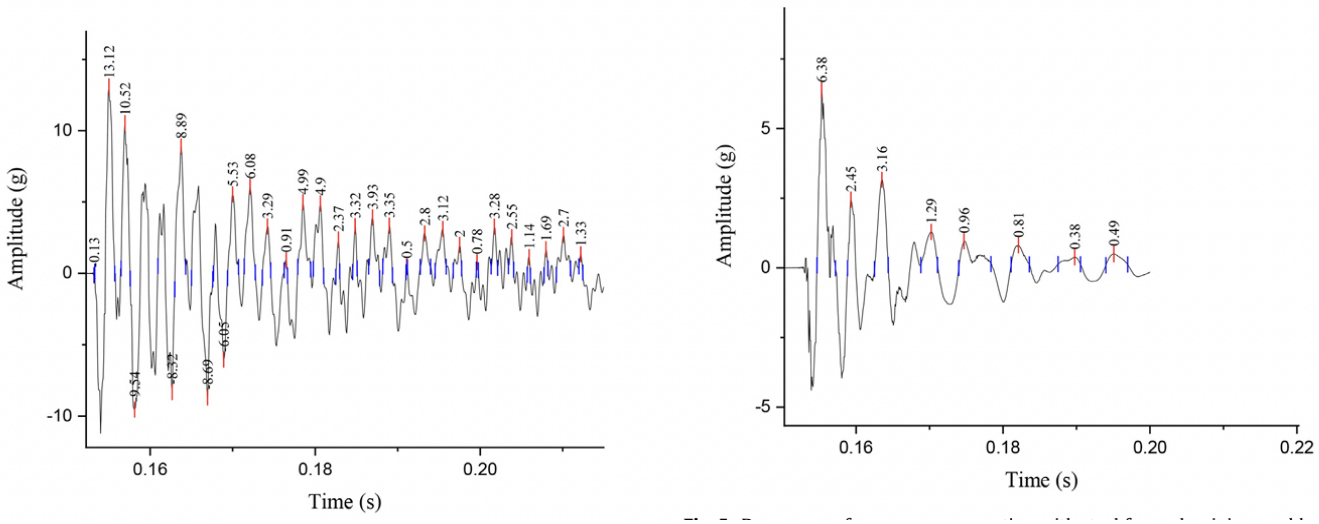

Figure 10: Damping curves for solid stainless steel (left) and the composite damper (right) [19].

Shock-Absorbing Mat System

The third and final design that was evaluated was a shock-absorbing mat system. This design places a dampening foam mat between the incubator and the stretcher, as shown in Figure 11. The mat is to be half an inch thick and have properties similar to the flooring of a weightlifting gym.

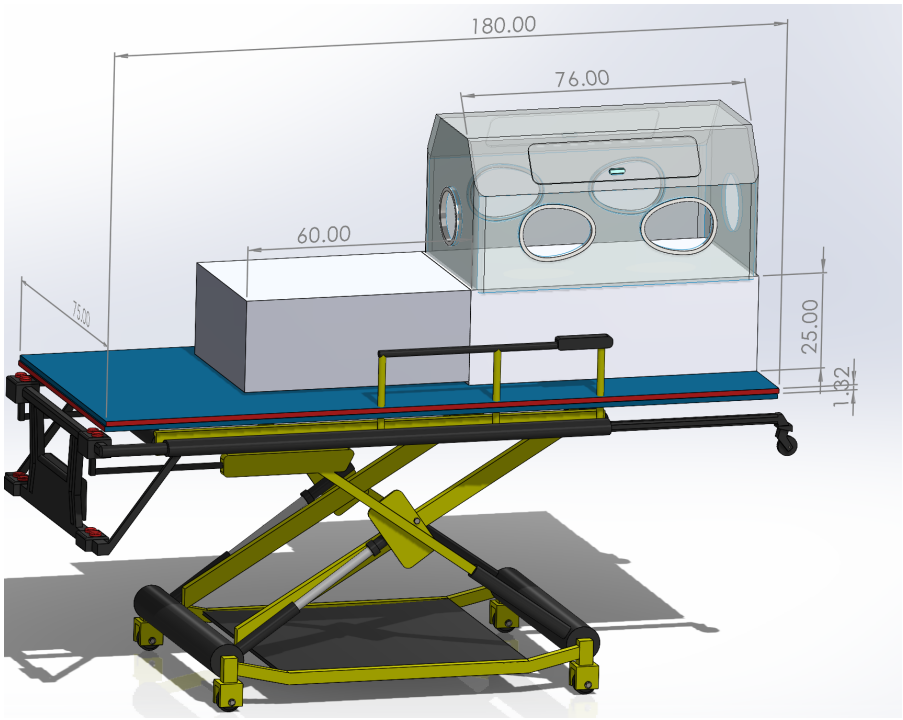

Figure 11: The entire incubator setup with the addition of the shock-absorbing mat system, which is shown in blue. All dimensions are in centimeters.

As of now, the standard stretcher and incubator setup only has padded areas where there is direct contact with the patient. A layer of high-density foam between the heavy incubator and the stretcher would ideally reduce the resonance of vibrations caused by hard metal and plastic components bumping into each other, thereby reducing whole body vibrations for the neonate during transport.

IV. Preliminary Design Evaluation

Design Matrix

In order to adjudicate which design would be the most effective, the team constructed a design matrix based on the most important considerations in the Product Design Specifications, which are fully outlined in **Appendix A**. Seven criteria were considered in the evaluation of the designs: safety, projected performance, compatibility, ease of fabrication, longevity, and cost. The results of this weighted analysis can be seen in Table 2.

One of the most highly weighted criteria was safety due to the high-intensity environment of the ambulance. The safety category assesses the potential for the device to cause harm or damage during both storage and use. Any mechanical, electrical, or chemical elements of the device must be hazard-free and easy to clean and sanitize for continuous use. For this reason, safety was weighted at 25.

The projected performance category assesses a device's ability to effectively reduce whole-body vibrations in neonates. The target is to reduce WBV to below 0.87 m/s^2 as recommended by the American Conference of Governmental Industrial Hygienists (ACGIH) [4]. This category was given a weight of 25 because it is an evaluation of a prototype's ability to reduce whole body vibrations. Any device that does not meet the performance requirements pose the risk of causing additional harm to the neonate.

The compatibility score predicts the device's ability to function without negatively impacting the travel incubator or any of the other equipment associated with the transport unit. Compatibility is a higher ranked category at 20 because the device should be easily integrable into the existing transport incubator setup; however, this is a secondary concern in comparison to safety and projected performance. Ideally, any potential designs would not require any significant modification to the existing transport system.

Ease of fabrication is defined in this context as the level of difficulty to create a working prototype of the design within the constraints of accessible materials, machinery, and time. Although the focus of this category is on small scale preliminary fabrication, the complexity of manufacturing on a larger scale could be factored into evaluation in this category as well. This category was given a weight of 15 because feasibility is an important consideration to ensure a testable prototype can be created. However, producing a device that effectively minimizes whole body vibrations is the ultimate goal and performance should be prioritized over simplicity.

The longevity category assesses the duration of the device's life in service. Since the frequency of neonatal transports at UW Hospitals is unpredictable, it is important that the device can be either stored for long periods without use or used continuously for many hours at a time. Although it is important for the device to last for many years, its rating was among the lowest since the projected performance of the device would determine whether the device provides a significant impact to justify replacing it over any period of time.

The cost category was scored based on the expenses of the materials as well as the cost to make the final product. As mentioned in the Product Design Specifications in **Appendix A**, all expenses of prototyping should remain under $500. The score for this criteria is less important to the client compared to safety and projected performance, and has mentioned that if the design were to cost more to be effective, the $500 budget has some flexibility.

Table 2: A design matrix comparing the three designs.

Design Categories (Weight)	**Magnet-Induced Levitation** 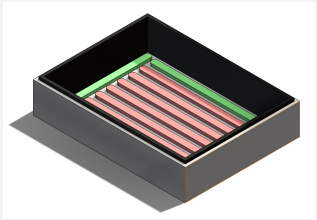		**Metal/Gel Composite Damper** 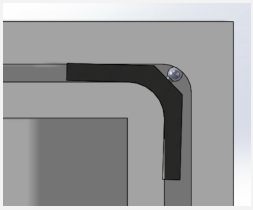		**Shock-Absorbing Mat(s)** 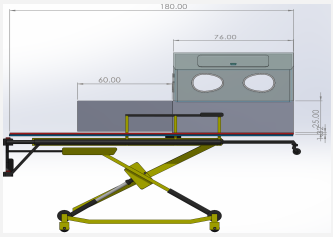	
Safety (25)	3/5	15	4/5	20	5/5	25
Projected Performance (25)	3/5	15	5/5	25	2/5	10
Compatibility (20)	2/5	8	3/5	12	4/5	16
Ease of Fabrication (15)	1/5	3	2/5	6	5/5	15
Longevity (10)	3/5	6	3/5	6	4/5	8
Cost (5)	4/5	4	3/5	3	3/5	3
Total Points:	51		72		67	

Design Evaluations

In evaluating the Magnet-Induced Levitation Device, it received a score of ⅘ in both safety and projected performance. The main safety concern was the potential for the repulsive force to excessively displace the incubator and create more forces that the neonate would

experience. Its score was deducted in the projected performance category due to the precision required to fabricate an effective device and for the potential variability in performance of the magnets after the device has been fully fabricated. The compatibility score was a ⅖ since hospital equipment and copious amounts of magnetic field are relatively incompatible. This device would be the most difficult to fabricate due to the need for the magnets to be placed with extreme precision. This is reflected in its score of ⅕ in the ease of fabrication category. Since magnets weaken over time, the device scored ⅜ with regard to longevity. The cost score was ⅘ due to the fact that magnets can be relatively inexpensive. Based on the scores assigned in the design matrix, this design scored an overall 51 out of 100 available points. Though this design is unique and innovative, there are significant barriers to the safe and successful fabrication and implementation of this design.

Evaluating the Magnet and Gel Composite Damper resulted in a safety score of ⅘. Close proximity to the neonate was the source of the deduction in an otherwise relatively safe design. points were awarded in the projected performance category due to the promising results of this composite's damping curve shown in Figure 10**.** The compatibility score for this design was a ⅜ due to the fact that it would take up space inside the incubator, which is extremely limited. Flight nurses, EMTs, and doctors that the team has consulted with have gone as far as saying modifying anything inside the incubator might be a non-starter. Fabricating this device will be challenging due to the need to ensure proper thicknesses of all materials on such a small scale. This awarded the design a ⅖ in the ease of fabrication category. The ⅜ in the longevity category was the result of concerns over the durability of the ball-and-socket joints under repeated and frequent use. Since all materials must be medical grade, this drives up the projected price and resulted in a ⅜ cost score. Overall, this design scored a 72 on the design matrix. This design takes into consideration the effectiveness of dampers in absorbing shock as well as the limited amount of space within the incubator to intervene with any kind of accessory.

The Shock-Absorbing Mat System was determined to be the most safe design, scoring a $^{5}/_{5}$. This is due to the placement of the mats on the stretcher itself, far away from possible contact with the neonate. It scored less well in the projected performance category due to the fact that the amount of vibrations that can be absorbed is limited to the thickness of the foam material. Only having half an inch of mat results in the deduction to a ⅖ score. As for compatibility, the device scored a ⅘ since the only impediment to the equipment's normal function is the chance of a slight

displacement due the decreased rigidity of the mat. This, however, is unlikely to have a significant impact. A $^{5}/_{5}$ in the ease of fabrication category was awarded due to the relative simplicity of the design, simply requiring the mats to be cut to the right dimensions. The device scored a ⅘ in longevity due to the durable but not indestructible nature of high-density foam mats. Assessment of costs required resulted in a score of ⅗ since a quality mat that would have all the characteristics the team is looking for would cost hundreds of dollars. Overall, the shock-absorbing mat design scored a 67 on the design matrix, placing it second on the team's evaluation list. The design scored well in several areas due its simplistic design and readily available materials. However, the predicted effectiveness and the cost of the materials revealed that this design may not be the most practical. It is possible that this design idea could be used in conjunction with another design and that the interaction between multiple vibration reducing designs could allow for the best possible solution to the problem at hand.

Proposed Final Design

After careful consideration of the factors in the design matrix and further research, the team decided to combine elements from multiple designs in creating the final prototype. This design consists of a metal and gel composite damper in a corner shape, as shown in Figure 12, and a straight shape, as shown in Figure 13. Together, these two components work to stabilize the neonate by reducing vibrations at three distinct points.

Upon further consideration after design evaluation, the pin joint element of the design was abandoned due to space constraints in the incubator. Instead, the device was measured and fabricated to fit snugly within the inner and outer trays without the need for any securing mechanism. In addition, the configuration of the damping layers was changed from a concentric layering to an iterating stacked pattern, as seen in Figures 12 and 14. This adjustment was made due to concerns about the feasibility of cutting layers thin enough to be arranged concentrically, and concerns that adhering the layers concentrically would be subject to significant human error. The stacked configuration still includes the same layers as the concentric configuration, but is more feasible to fabricate.

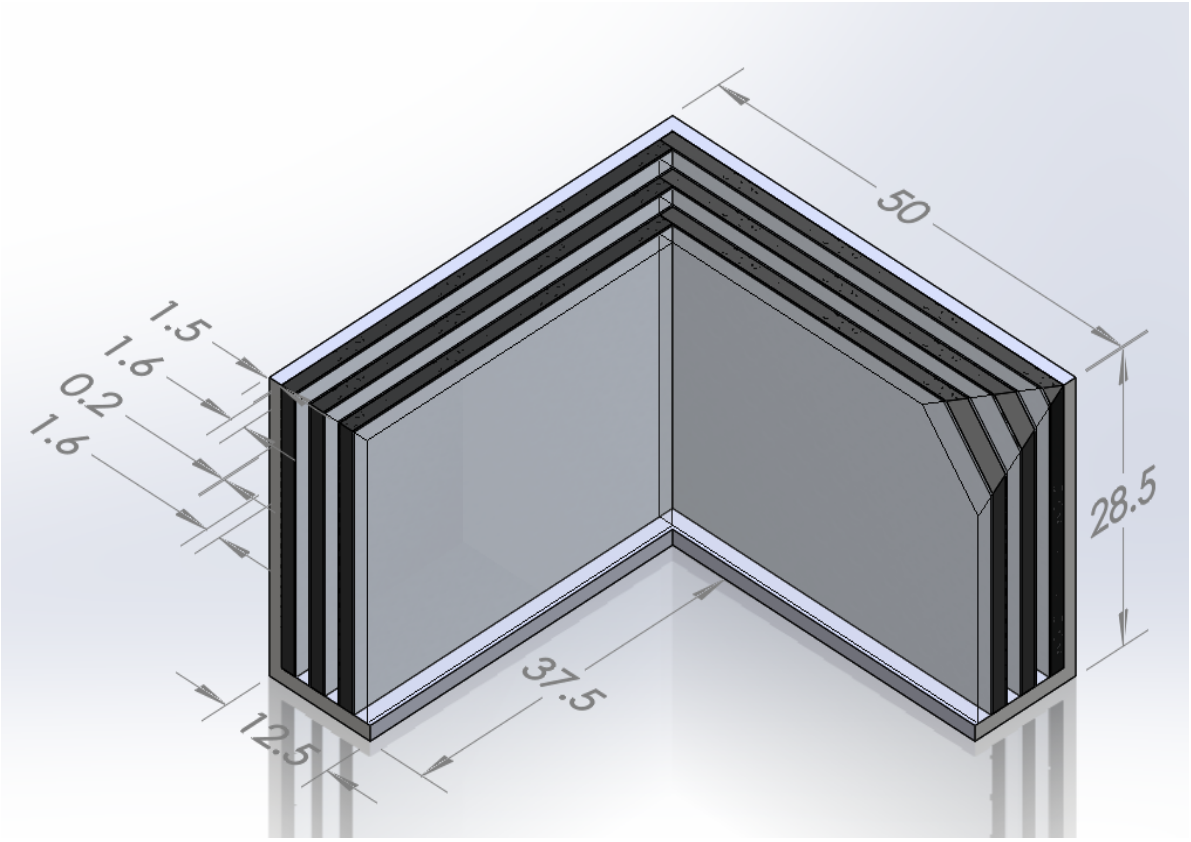

Figure 12: View of proposed corner damper with stacked layer configuration, with dimensions in millimeters. On the upper right corner, there is a triangular section removed so that the layers can be better visualized.

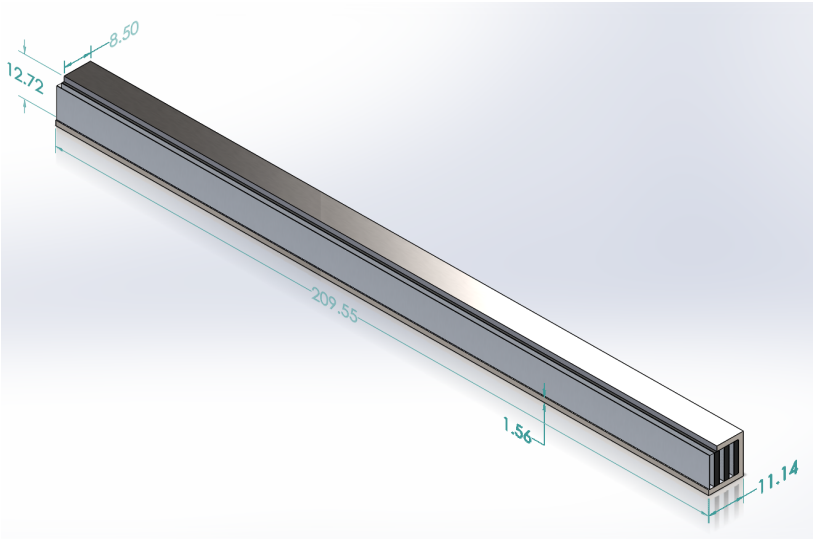

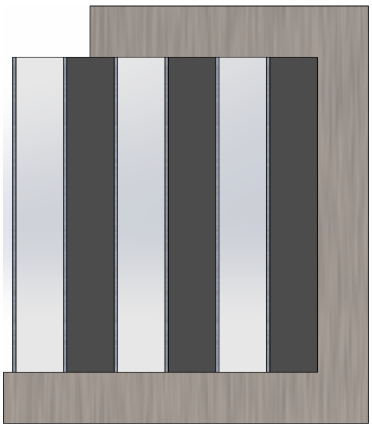

Figure 13 (left) and Figure 14 (right): View of proposed side damper, with dimensions in millimeters.

V. Fabrication/Development Process

Materials

The device consists of an iterating pattern of stacked shock-absorbing layers. The layers are configured in a stacked pattern within a stainless steel tube: first, a layer of foam; second, a layer of aluminum foil; third, a layer of silicone gel; and fourth, another layer of aluminum foil. All materials ordered were within the client's budget constraints. A materials and cost list to fabricate the Metal/Gel Composite Damper can be found in **Appendix B**.

The outermost layer of the device is made from stainless steel, which encases all of the aforementioned layers on two sides on the L-shaped corner dampers, and three sides on the side dampers. The corner dampers are L-shaped, with a height of 28.5 mm, length of 37.5 mm on each side of the corner, and width of 12.5 mm on the bottom face. The side damper, which is straight, is 12.72 mm tall, with walls 1.56 mm thick. The stainless steel layer is meant to emulate the beak of a woodpecker, which can withstand any direct and forceful impacts. Steel was also chosen to be the outermost layer because it is easy to sterilize in a medical setting. Utilizing the dimensions of the straight damper, a spring constant for stainless steel was calculated to compare the elastic properties of stainless steel to the woodpecker's beak structure [20]. This was done using Equation 1 in which the stainless steel component of the straight damper was idealized to a rectangular sheet sheet with dimensions of 8.25 in. x 0.50 in. x 0.065 in. (209.55 mm x 12.7 mm x 1.651 mm) [20]. In Equation 1, k is the spring constant, A is the cross-sectional area, E is the Young's Modulus, and l is the length of the sheet. The Young's Modulus for stainless steel was obtained from published values [21]. All values were converted to SI units.

$$k_{steel} = \frac{A_{steel} * E_{steel}}{l_{steel}} = \frac{(2661.285\ mm^2) * (1.90E5MPa)}{209.55\ mm} = 2.413E6\ N/mm = 2413\ N/m \quad (1)$$

Published or experimental values for the damping coefficient or ratio of stainless steel could not be found, so the average value for metals in their elastic deformation range was used. Below their yield point, metals typically exhibit a damping ratio of around 0.01 which is

somewhat different from the experimental damping ratio of 0.032 employed for the beak. However, both ratios fall into the qualification of "low" damping ability.

A layer of foam was the first layer in the pattern to be adhered within the stainless steel. This foam sheet is 1.6 mm thick [22]. The foam will act as a first line of defense in damping the vibrations of transport, and mimics the characteristics of a woodpecker's hyoid, which supports its tongue, used to block vibrations from penetrating further within the skull. The material properties of the foam were evaluated using the same approach described for stainless steel. All literature values used were for nitrile rubber, as this was the major material in the foam used [23]..

$$k_{foam} = \frac{A_{foam} * E_{foam}}{l_{foam}} = \frac{(2661.285\ mm^2) * (0.855\ MPa)}{209.55\ mm} = 10858.5\ N/mm = 10.859\ N/m \quad (2)$$

Published values for the density and damping ratio were used to calculate the damping coefficient of the nitrile rubber/foam chosen for the second layer. Materials with high damping coefficients are able to dissipate vibrational energy to a greater extent, returning the vibrational frequency distribution to the resting value more quickly. In Equation 3, c is the damping coefficient, ζ is the damping ratio, m is the mass, and k is the spring constant calculated in Equation 2.

$$c_{foam} = \zeta * \sqrt{m_{foam} * k_{foam}} = 0.1 * \sqrt{5.04E-3\ kg * 10.849\ N/m} = 0.023\ N\,s\,m^{-1} \quad (3)$$

A comparison could be made between the damping ratios of nitrile rubber and the hyoid. Published literature values concluded a high damping ratio of 0.25 for the hyoid, while the published damping ratio for nitrile rubber was 0.1. Although this is significantly different from the value for the hyoid, this was deemed acceptable because the nitrile rubber still demonstrated dampening properties.

The foam layer was followed by a layer of aluminum foil. The foil acts like the woodpecker's skull with cerebrospinal fluid, which is rigid and has little space for fluid to transmit vibrations. Once again due to size constraints, aluminum foil is the thinnest option to put between the foam and silicone layers. Aluminum foil is also inexpensive to purchase. The

ability of aluminum foil to emulate the function of the skull bone was evaluated using Equation 4 to obtain the spring constant and by comparing the published damping ratios for each [24].

$$k_{alum} = \frac{A_{alum} * E_{alum}}{l_{alum}} = \frac{(2661.285\ mm^2) * (7E4\ MPa)}{209.55\ mm} = 889000\ N/mm = 889\ N/m \quad (4)$$

Both aluminum and the skull bone with CSF act as primarily elastic materials, with damping ratios of 0.01 and 0.032 respectively. This indicates that the two materials would likely respond similarly to applied forces [20].

The next layer in the arrangement is a sheet of silicone that is 1.6 mm thick. This layer has a durometer value of 40, which is about the hardness level of a gel shoe insert. As the innermost layer, this silicone attempts to mimic a woodpecker's spongy bone, which can dissipate mechanical vibrations before they penetrate further. One key component of the spongy bone that allows it to do this is the ability of the spongy bone to act as a low-pass filter. The spongy bone allows low frequency vibrations to pass through but absorbs more destructure, higher frequency vibrations. This key component is related to the porosity of the spongy bone [20]. A sheet of this thickness was used due to the size constraints of the device, as the device must fit within the 11.3 mm space between the inner and outer trays of the incubator. The ability of the foam to emulate the function of the spongy bone was evaluated using the same approach as the other materials by calculating the spring constant in Equation 5 and comparing published damping ratios.

$$k_{gel} = \frac{A_{gel} * E_{gel}}{l_{gel}} = \frac{(2661.285\ mm^2) * (1.30E5\ MPa)}{209.55\ mm} = 1.651E6\ N/mm = 1651\ N/m \quad (5)$$

A published experimental study obtained damping ratios that ranged between 0.058 and 0.077 [25]. No direct comparison could be made between the material values for silicone and the spongy bone because an empirical method was used to evaluate the spongy bone in S.H. Yoon's study [20].

Methods

The steel housing for the L-shaped corner damper was produced from a 0.057 in. (1.448 mm) thick, 12 in. x 12 in. (304.8 mm x 304.8 mm) stock sheet. The stock was cut into 3.7 in. x 1.4 in. (93.98 mm x 35.56 mm) sections and in the center along the long side of the rectangle an isosceles triangle cut-out with a base of 0.8 in. (20.32 mm) and a height of 0.4 in (10.16 mm) was formed using a water jet. To create the L-shape from the flat section, the stainless steel sections were bent 1.8 in. (45.72 mm) into the 3.7 in. (93.98 mm) side using a sheet metal bending break to form a 90° angle. Then, the piece was bent again, but 0.4 in. (10.16 mm) into the piece in the shorter direction to create a base. These steps were completed twice, to create two total corner dampers.

A hollow, rectangular tube with the dimensions 36 in. x 0.5 in. x 0.5 in. (914.4 mm x 12.7 mm x 12.7 mm) was used to produce the steel housing for the straight, side dampers. The tube was cut to a length of 8.25 in. (209.55 mm) using a bandsaw. One face of the tube was removed using a mill to create an opening through which the other three material layers could be inserted. After one side was removed, one exposed side was milled down an additional 0.09 in. (2.286 mm). The gap between the inner and outer trays is larger on the bottom due to walls of the inner tray being slanted, so the difference in widths ensures that the damper can fit flush with the tray.

Finally, the layers were cut to size and assembled in the previously described iteration pattern. The first layer in the pattern, foam, was cut from a stock sheet. Three strips were cut matching the length and width of the outer steel housing for the side dampers. To reduce the thickness and create the necessary six total foam layers, the thickness of each of the three strips were cut in half using a utility knife. From the stock sheet, six more rectangular layers were cut and thinned to match the two vertical faces of the corner dampers. The next layer in the pattern, aluminum, was cut using scissors to the same length and width as the foam layers from a roll of aluminum foil. Six total aluminum strips were made for the side dampers and 12 total aluminum segments were made for the corner dampers. The final material, silicone, was cut from a stock sheet. Scissors were used to create the same number of individual layers with the same dimensions as the foam and aluminum layers described above.

To assemble the straight dampers, a layer of spray adhesive was applied to the inner wall of the steel housing that opposes the removed face. The first layer of the pattern was placed against the steel wall, compressed, and allowed a short time to dry. Subsequent layers were

attached face-to-face with spray adhesive applied between each. This was repeated until three iterations of the pattern were complete and the last layer of silicone extended just past the steel housing. The assembly of the corner dampers was very similar in that adhesive was applied first followed by the addition of another layer in the pattern. Two separate segments of each layer were added at a time to cover both vertical faces of the corner dampers. The layers were added outward until the pattern extended past the horizontal face. Any extra material extending past the lengths of the corner dampers or side dampers were trimmed using tin snips to create neat ends. A formal and detailed fabrication protocol can be found in **Appendix C**.

Final Prototype

Figure 15: A trimetric view of one of the side dampers with one section of the foil exterior removed. Dimensions are in mm.

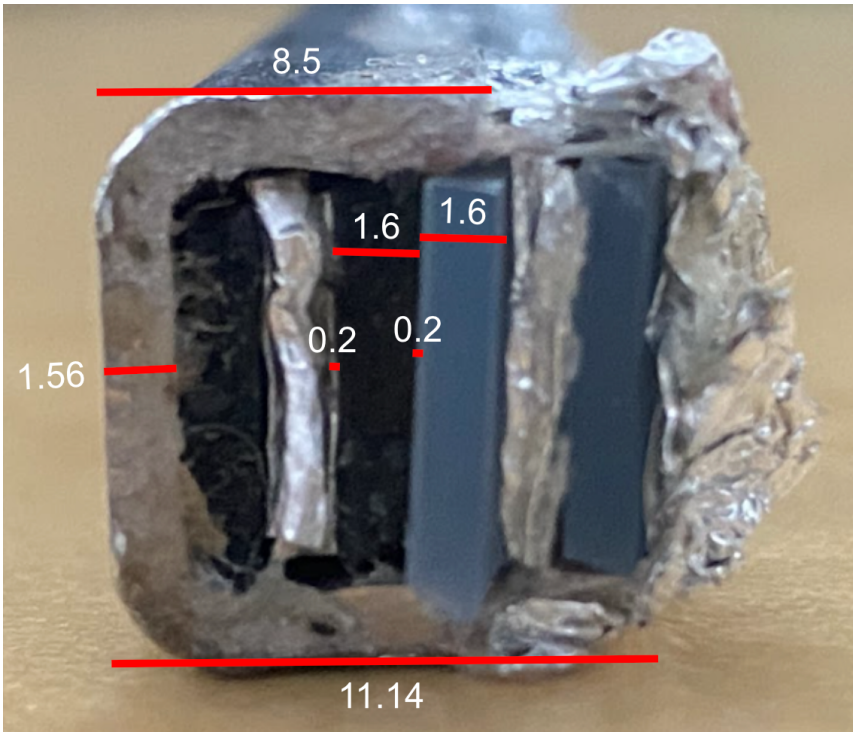

Figure 16: A side view of one of the side dampers with a section of the foil exterior removed such that the damper layers are visible. Dimensions are in mm.

The side dampers were successfully fabricated as envisioned using the repeated layers of foam, foil, and gel. They fit snugly in the steel housing and are encased in a layer of aluminum foil. Figure 15 shows the entire side damper prototype, while a more detailed cross-sectional view is available in Figure 16. The side of the damper that is covered with foil is to be placed flush with the outside of the inner tray, while the steel housing should rest against the walls of the outer tray.

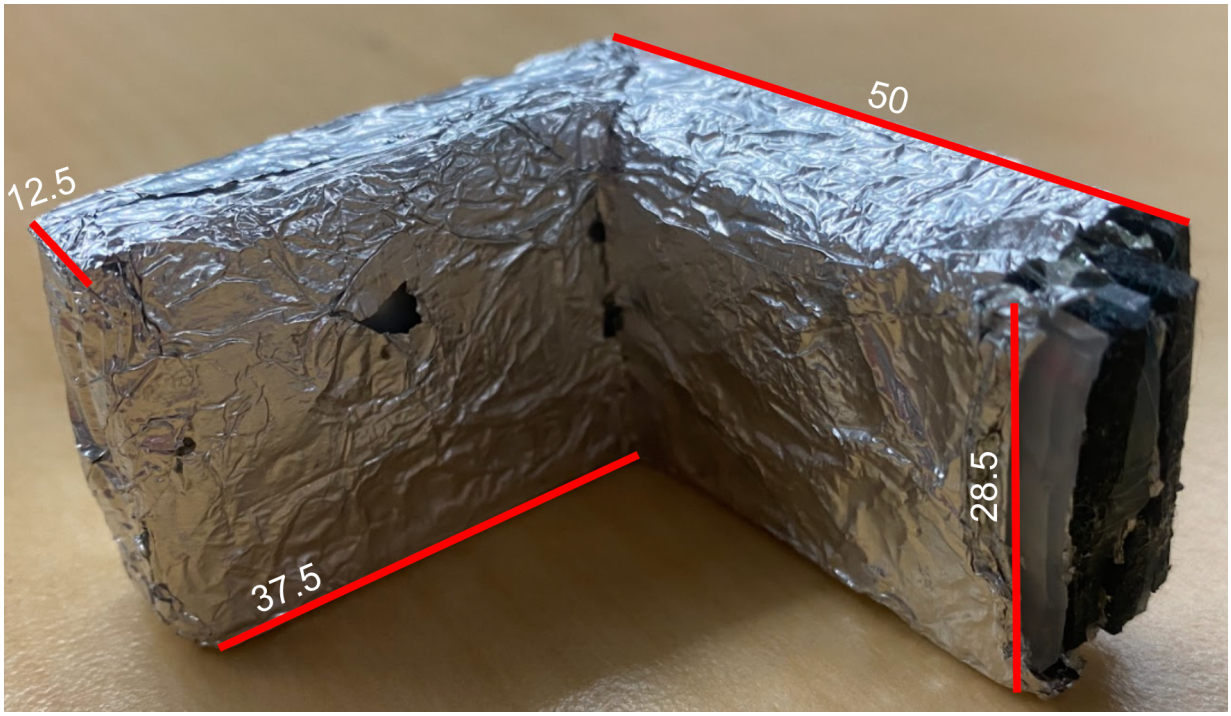

Figure 17: A trimetric view of one of the corner dampers with one section of the foil exterior removed. Dimensions are in mm.

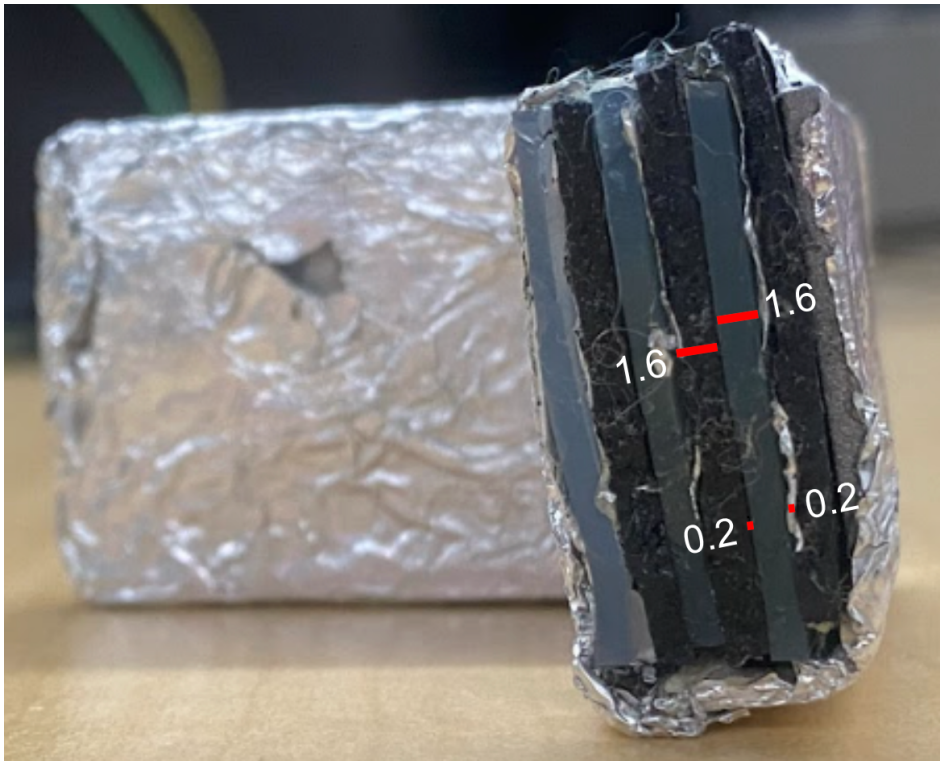

Figure 18: A side view of one of the corner dampers with a section of the foil exterior removed such that the damper layers are visible. Dimensions are in mm.

The corner dampers were also successfully fabricated as envisioned with the repeating layers of foam, foil, and gel. The layers are flush with the bottom of the steel housing and are pressed snugly against each other. Figure 17 shows a view of the entire corner damper, while Figure 18 shows a more detailed view of the layer cross-section.

Figure 19: All four dampers laid out in a similar configuration to how they would be arranged in the incubator.

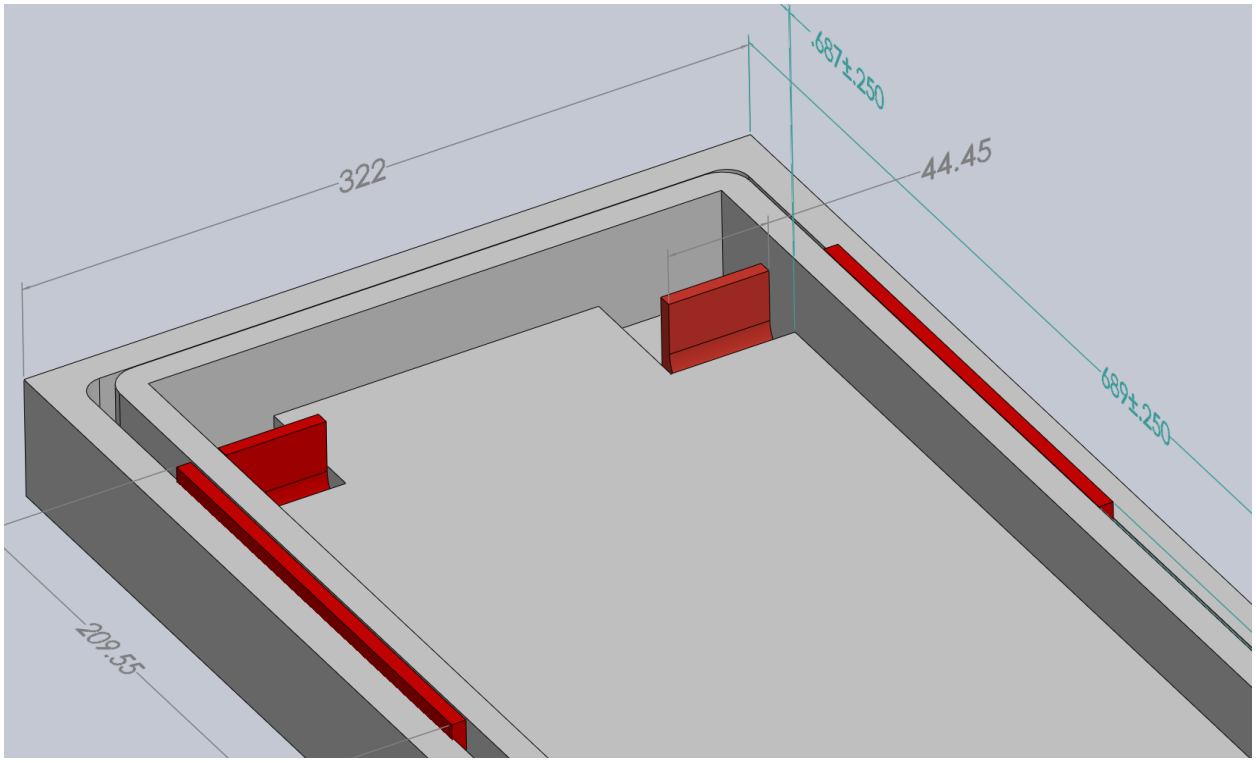

Figure 20: A trimetric view of the damper placement configuration within incubator trays.

It was initially proposed that the corner damper would be placed such that the bottom of the steel housing would be L-shaped and follow the corner between the inner and outer trays. However, the location of the corner dampers was slightly modified from the original design due to size constraints. Instead of the corner dampers being placed at the corners between the inner and outer trays, they were placed upright in holes in the corners of the inner tray, with one side of the damper underneath the inner tray and one side protruding from the ventilation hole in the corner of the inner tray. This configuration can be visualized with the prototypes in Figure 19 and modeled in SolidWorks in relation to the inner and outer tray in Figure 20.

Testing

To obtain baseline measurements, the team scheduled a ride in the ambulance with the UW Hospital Med Flight Team to record vibrations present in the current transport setup without the dampers. The team designed an approximately 40 minute route for the ambulance consisting of a highway, main roads, heavy traffic areas, low traffic areas, stop lights, stop signs, bumps,

sharp turns, hills, and various speed limits (Fig. 21). The UW Med Flight team completed the route using typical driving practices so that the test run could be as similar as possible to a normal transport. Six phone sensors were taped securely to various locations in the ambulance. The team placed one device on the head and one on the chest of an infant mannequin within the incubator as shown in Figures 23 and 24, two more at the middle and back of the stretcher deck, and two more on the floor at the front and back of the stretcher as shown in Figure 22. Data was recorded continuously throughout the drive. In order to correlate and contextualize the data collected, an event log was taken during the trip with exact timings of events such as accelerations, bumps, hills, hard stops, and turns.

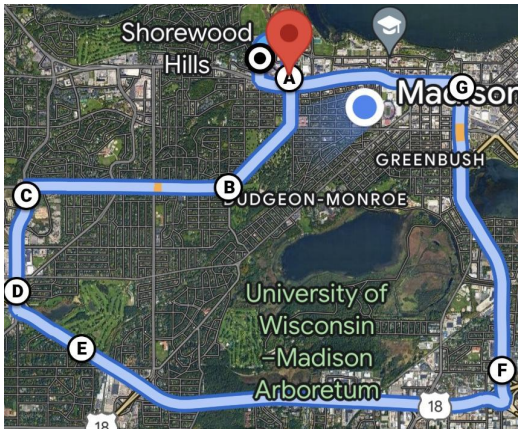

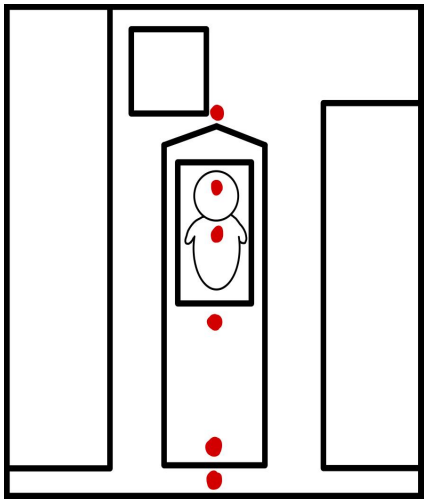

Figure 21 (left): A map of the first route that was tested which included a variety of road types and obstacles.

Figure 22 (right): A diagram showing the locations (in red) of sensors used for data collection in the ambulance during testing.

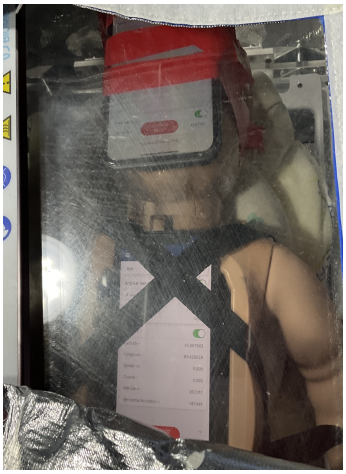

Figures 23 (left) and 24 (right): Two views of the infant mannequin in the incubator with phones attached.

In order to test the ability of the dampers, a second ride in the ambulance was conducted with the dampers in place. The side dampers were placed between the inner and outer trays with the stainless steel housing placed against the outer tray and the shock-absorbing layers facing towards the inner tray. The corner dampers were placed upright in the corner holes of the inner incubator tray. Data was collected using the same six phones in the same locations and orientations throughout the ambulance. The sampling frequency and chosen sensors were constant throughout the baseline and final test runs. An event log was taken in the same fashion as the baseline test run.

The test run with the dampers was conducted using a slightly different route than the baseline test run. The route was extended and modified to include the interstate highway, at which the ambulance travels at speeds of 70-80 mph. This modification allowed an analysis of any variation in prototype performance as travel speeds increase. Another slight variation in testing conditions between the baseline measurement run and the test run was traffic conditions; the baseline run was conducted between 3:00 and 4:00 PM on a Friday, and traffic was considerably higher than the test run, which was conducted between 12:30 and 1:30 PM on a Friday. This difference in traffic conditions resulted in more hard stops and accelerations during the baseline run than during the prototype testing run, as reflected in the event logs for each run.

Data collection was completed using the accelerometer and gyroscope built into each team member's phone. The "MATLAB" application can measure acceleration in the x, y, and z directions. It recorded linear acceleration, angular velocity, position, and orientation values. The app can also remember the maximum and minimum values for a period of time which were necessary for the calculations of the PSD curve. The devices were placed strategically, as described above, in order to cover the greatest area for the generalization of a PSD value for a given space. Notably, the mannequin used for testing was made of soft plastic, and was much larger than a typical neonate that would be transported.

The team measured the strength of vibrations for the chest and head of a neonate mannequin within the incubator, the floor of the transport vehicle, and the deck of the transport unit as a measure of the Power Spectral Density. The PSD is a measure of the mean square acceleration per unit of bandwidth and can be used to evaluate the randomized vibrations that occur during transport [19]. The shape of a Power Spectral Density plot can be used to define the mean acceleration of a random signal at any frequency. The area under the plotted PSD curve is the mean square (g^2) of the signal and the square root of the graphed area is the acceleration's overall root-mean-square (RMS) value (σ) [18], [20].

The chosen testing methods will determine whether the damper prototypes meet design specifications by comparing experimental measurements to literature values (0.87 m/s^2) which describe the maximum vibrations allowable for patient safety. The testing methods will also provide comparisons between the power of vibrations in the baseline and final tests as an indication of improvement. Experimental data can be converted to acceleration versus time graphs as well as PSD curves to create comparable values to determine success. The expected outcome is that the dampers lower all vibrations throughout the final test run to amplitudes lower than the literature value. In terms of the power of vibrations, it is expected that the dampers reduce overall power from baseline to final measurements. Results that indicate all vibrations are lower than 0.87 m/s^2 are considered successful and results that show vibrations above 0.87 m/s^2 are considered unsuccessful.

VI. Results

The acceleration data acquired from the testing runs was uploaded to MATLAB drive. A Discrete Fourier Transformation was applied to the total magnitude of the acceleration data to gather the frequency information. An analysis of the frequency derived from the transform was done to provide information about the vibrations experienced by the neonate mannequin inside the isolette as well as the surrounding setup. The data was cleaned using the detrend function in MATLAB to remove the best straight-fit line [26]. The sensors were grouped by location for analysis; the four sensors outside the incubator during baseline testing were grouped together, the two sensors inside the incubator during undampened baseline testing were grouped together, and the two sensors inside the incubator during dampened device testing were grouped together. These groups were formed so that performance of the damper could be compared to vibrations experienced inside and outside the incubator during a standard transport trip. Acceleration magnitude was plotted with respect to time in Figures 25, 26, and 27 below. Power spectral density graphs were created for each of the three sensor groupings in Figure 28. The MATLAB code and raw data can be found in **Appendix D**. Qualitative size comparison of the spectrums in Figures 28 (A) and (B) from baseline testing suggests that a large amplification of vibrations occurs inside the incubator within the 0 to 20 Hz range.

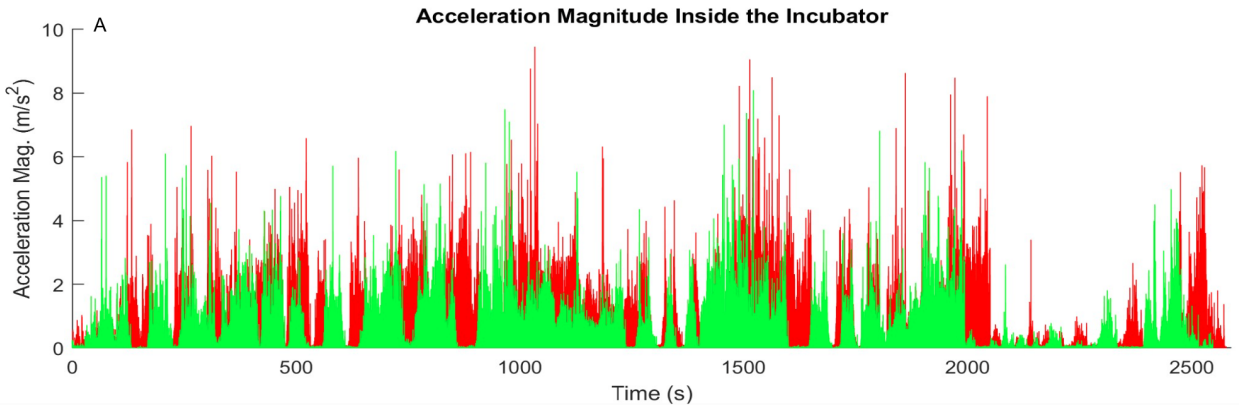

Figure 25: An acceleration vs. time plot for the head and chest sensors during baseline testing. The red peaks represent data collected from the head and the green peaks represent data collected from the chest of the infant mannequin.

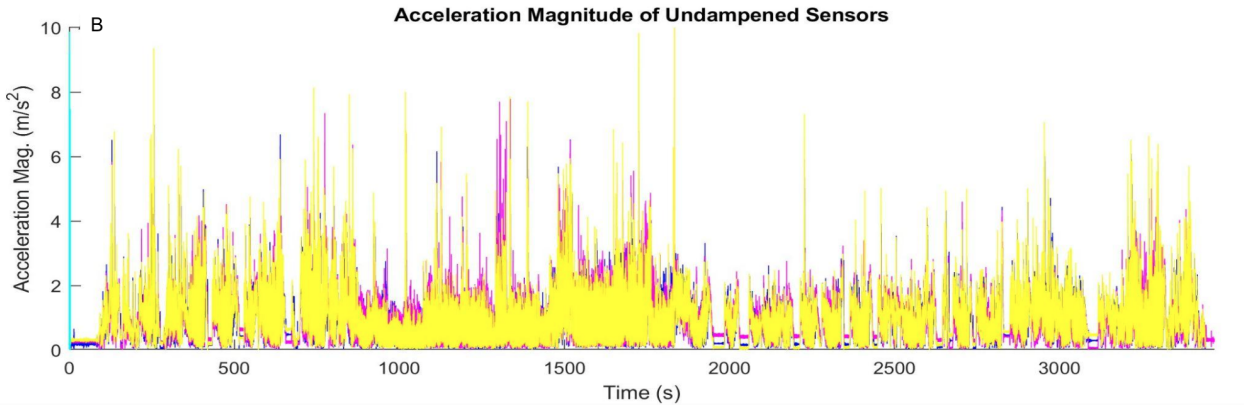

Figure 26: An acceleration vs. time plot for the four undampened sensors placed outside the incubator on the sled and floor of the ambulance. The yellow peaks represent data from the back floor, magenta is the front floor, blue is the middle of the sled, and cyan is the back of the sled.

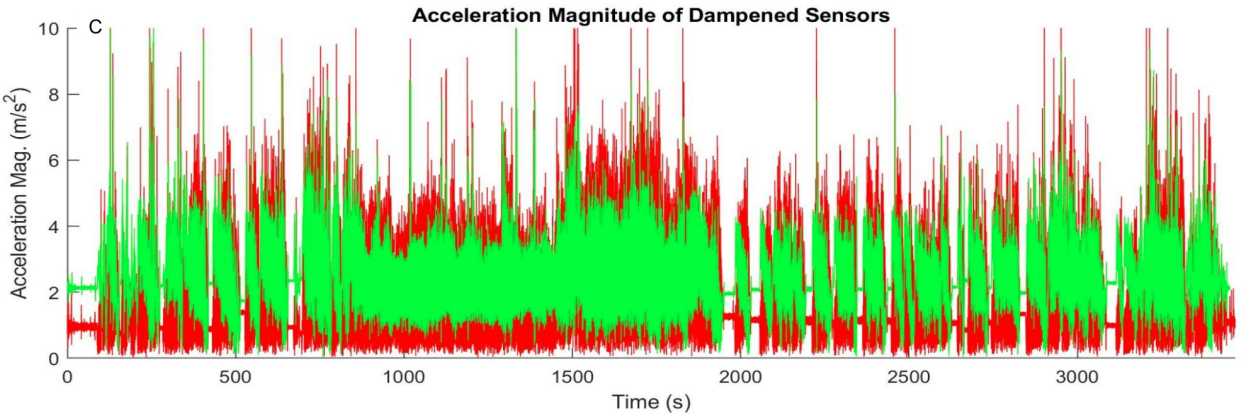

Figure 27: An acceleration vs. time plot for the head and chest sensors during device testing. The red peaks represent data collected from the head and the green peaks represent data collected from the chest of the infant mannequin.

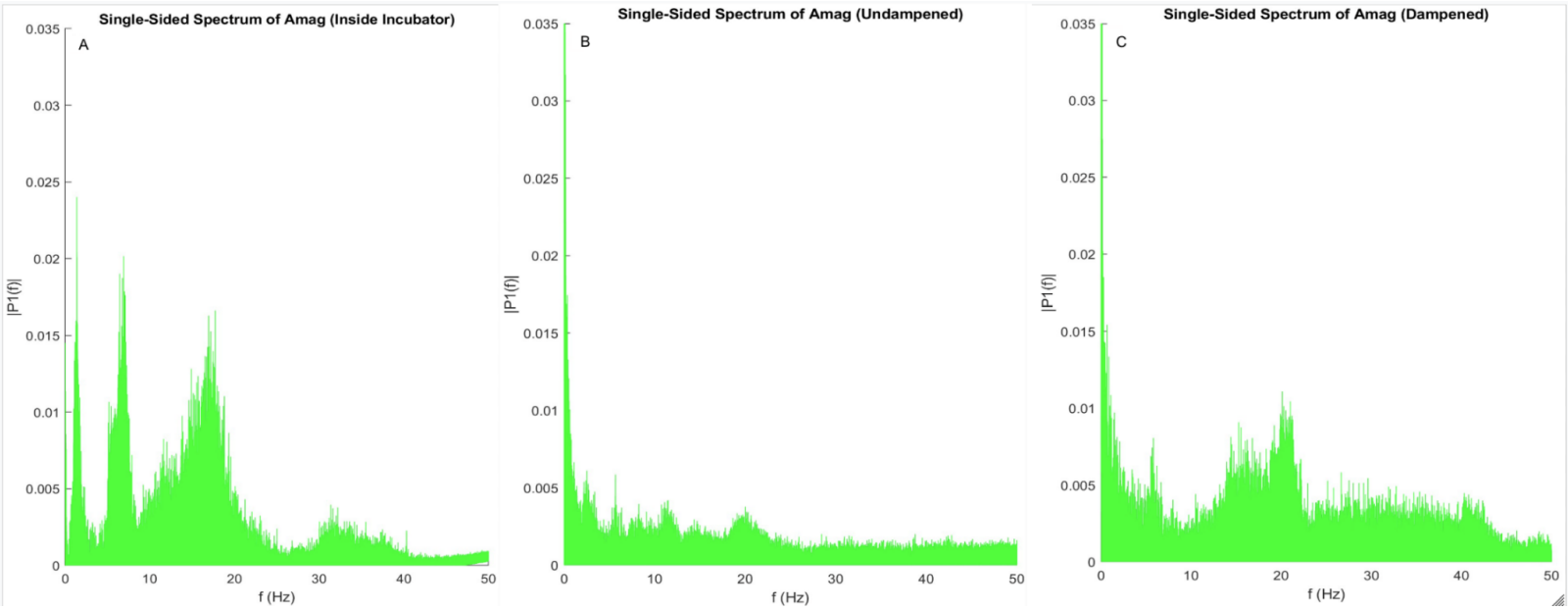

Figure 28: (A) A power spectral density graph for the frequency data gathered from sensors inside the incubator during baseline testing. (B) A power spectral density graph for the frequency data gathered from sensors outside the incubator during baseline testing. (C) A power spectral density graph for the frequency data collected from sensors inside the incubator during device testing.

To increase the number of trials conducted for data analysis, acceleration vs. time data was binned into one minute intervals. The fourier transform was applied to each bin and the power spectral density data was once again binned using step sizes of 1 Hz ranging from 1-50. Peaks at each frequency value were determined by averaging the step sizes of 0.0166 Hz within each frequency bin. A t-test was run for each frequency bin comparing the dampened frequency peaks inside the incubator to the undampened frequency peaks outside the incubator. Since multiple t-tests were run for each sensor combination, the Bonferroni correction was implemented to lower the threshold of significance for the obtained p-values as calculated in Equation 6 [27]. The amount of times that a combination of sensors produced a significant p-value at any of the frequencies was counted and plotted in Figure 29 using the p-value table in **Appendix E**.

$$\alpha^{*} = \frac{\alpha}{\left(\frac{k}{2}\right)} = \frac{0.05}{750} = 0.0000667 \qquad (6)$$

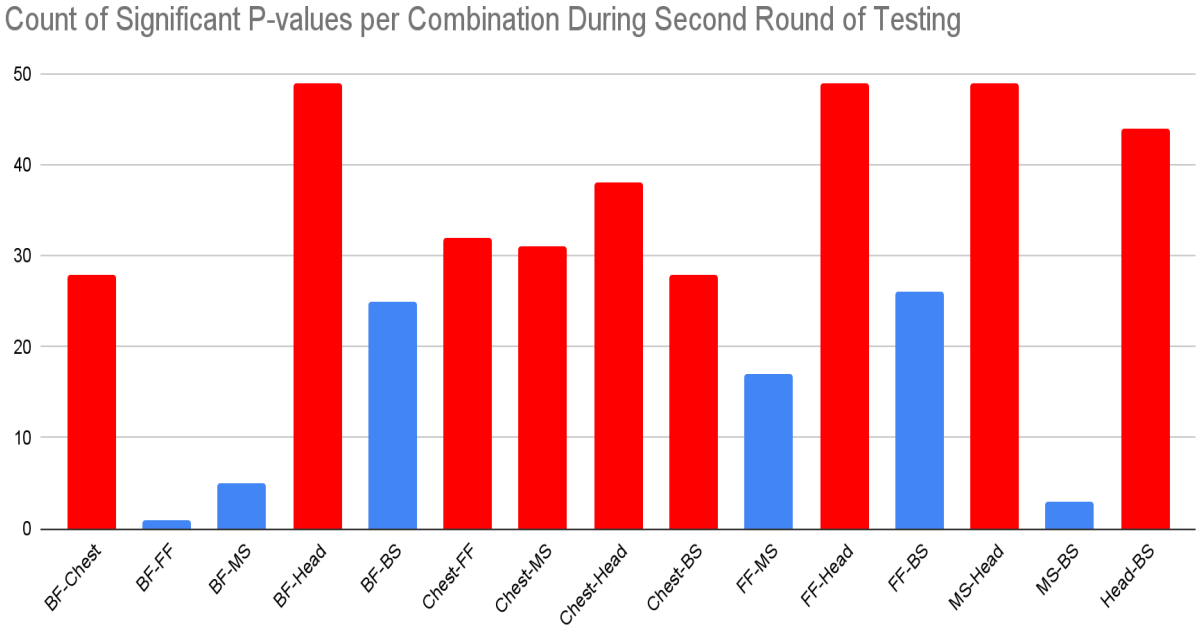

Figure 29: The count of significant p-values that reached the α threshold during the second round of testing. A red bar denotes comparison of a dampened sensor to an undampened sensor, while a blue bar indicates that two undampened sensors were compared.

More significant p-value comparisons were found when a dampened sensor was present. A similar statistical analysis was performed, this time for the sensor combinations of chest and head from the baseline and testing runs. Another Bonferroni correction was implemented, the alpha for which is calculated in Equation 7. The p-values were again counted and their significance counts are plotted in Figure 30 using the p-value table in **Appendix E**.

$$\alpha^{*} = \frac{\alpha}{\left(\frac{k}{2}\right)} = \frac{0.05}{200} = 0.00025 \tag{7}$$

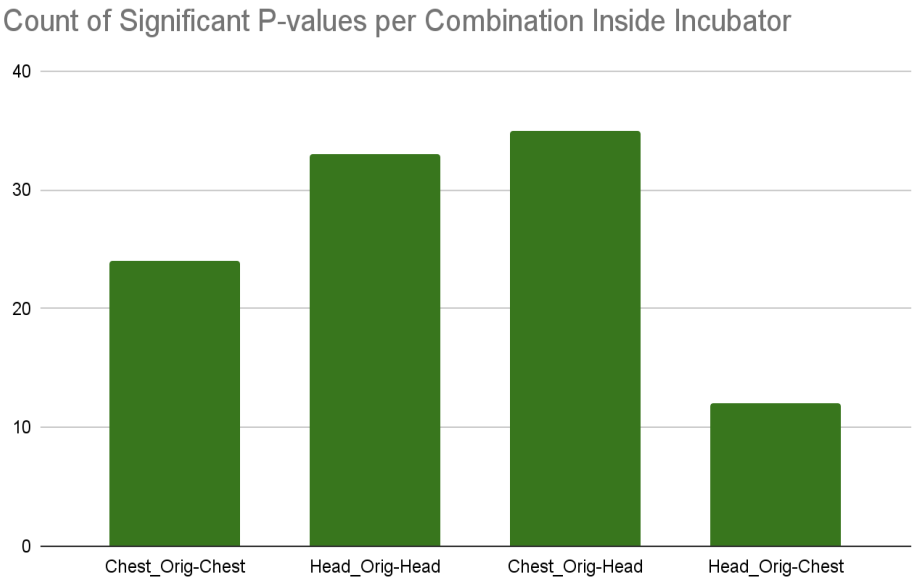

Figure 30: A bar chart tracking the amount of times that a p-value was significant comparing the sensors inside the incubator during baseline and testing runs.

The p-values were significant for the chest comparisons 24 out of 50 times and the head comparisons were significant 33 out of 50 times. There was a significant reduction in vibration inside the incubator when the prototype was installed as seen on the spectrums in Figures 28 (A) and 28 (C). The powers around 7 Hz and 17 Hz were significantly reduced and the energy was dissipated into surrounding frequencies as seen in the flatter trend when using the prototype. The average acceleration inside the incubator was calculated to be 2.19 m/s^2. Refer to **Appendix F** for the complete table of acceleration values.

VII. Discussion

Implications of Results

After testing the device to see how it would respond to a transport ride complete with all of the necessary transport equipment, the team was able to draw several conclusions related to the information collected and the efficacy of the design. Firstly, after conducting our experiments and analyzing the results, our team noticed a significant difference in the power observed inside the isolette when using the dampening prototype compared to when not using the prototype. This

difference is evident in the graph of the spectrum, which shows a reduction in the peak power levels at the 7 Hz and 17 Hz ranges when using the prototype (Fig. 28 (A) and 28 (C)). Additionally, our calculated p-values indicate that this difference is statistically significant, especially in the range of 5-25 Hz. This reveals that the use of the prototype had a real and measurable effect on the power levels inside the isolette. This suggests that our prototype is capable of reducing whole-body vibrations during neonatal transport by dispersing vibrations across a range of frequencies as expected from the performance of a damper. While frequencies ranging from 10-20 Hz can be beneficial to development [28], the prolonged nature of the event can increase the stress on the neonate.

The second comparison the team noticed was the drastic difference in the power of the spectrum inside the isolette compared to outside the isolette. Many would imagine that an isolette would reduce the power since it is responsible for holding the critically ill neonate; however, the power was greater by an average of 3x for each frequency bin that was analyzed (Fig. 25). The p-values indicate that the comparison of sensors inside the isolette with the sensors outside of the isolette were significant as often as 49/50 times (Fig. 28). This data exacerbates the need for a solution to the problem and further clarifies that existing equipment does not provide any dampening benefits and instead amplifies the vibrations in the ambulance.

Finally, the calculated average acceleration value of 2.19 m/s^2 is significantly higher than the accepted literature value of 0.87 m/s^2 [4]. This indicates that the prototype was not effective in reducing the acceleration inside the incubator to the degree that was required by the PDS (**Appendix A**). Despite the prototype's attempts to reduce the frequency levels, they remained above the threshold set in the specifications, indicating that the prototype did not meet the desired performance standards. Reducing the power of a frequency would mean that the frequency carries less energy and would lead to a decrease in the magnitude of acceleration for an object. Acceleration is a measure of the rate of change of velocity of an object, and is determined by factors such as the mass of the object, the force applied to the object, and the object's resistance to the force. A damper does not directly affect any of these factors, so modifying the damper would not necessarily affect the acceleration of an object. Therefore, additional components to the final design should be sought in order to meet the expectation to decrease acceleration.

Due to the fact that the 0.87 m/s^2 threshold was not reached as specified in the PDS, alterations must be made to the design. Future iterations of the design will be aimed at shifting the power to a lower range of frequencies such as 0-10 Hz in order to provide the neonate with a natural vibration that is reminiscent of its mother's body [26].

Ethical Considerations

In the development of a new medical device, ethical considerations must be addressed in regards to research, patient safety, and inclusivity. First, ethics surrounding medical research involves acting on sufficient information and understanding and using that information to promote well-being [29]. The quantity and quality of research must be sufficient in providing an accurate, complete description of the problem and design variables in order to make informed decisions. Understanding of the research is just as critical as the team needs to act as experts in the identified field. A final focus of research ethics is reporting the research honestly and giving credit where it is due. Medical devices operate on the basis of the truth of the research done and will inevitably fail if research is falsified.

Secondly, medical ethics address the importance of patient safety and health through official device approval and testing. It is important to prove device efficacy prior to use to ensure that the device will function as intended. To do so, the device must comply with the standards set for Class II medical devices according to the FDA and receive approval prior to use [30]. Additionally, the use of steel as the outer layer of the dampers ensures that the device meets all biosafety requirements for medical devices, as it can be easily removed and sterilized using an autoclave or ethylene oxide [31]. In regards to testing, it is important that results are reported transparently and all results are included. Omitting negative test results falsely informs clients and patients about device efficacy and can result in device failure during use.

Finally, inclusivity is an important ethical consideration which allows all patients to have the access and ability to use the device. Thus, religious, cultural, and economic considerations were taken into account during development of the final prototype. The chosen materials are permitted among all known cultures and religions which may forbid the use or interaction with certain substances. Finally, the cost of the device is kept low to allow accessibility to clients and patients regardless of economic status. Ethical considerations were taken into account throughout the design process and guided decisions to create a well-informed prototype.

Sources of Error

Several sources of error need to be considered in order to identify inconsistencies and limitations in accuracy. One such source of error is during fabrication, the foam mat layers were cut in half along the thin edge using an X-Acto knife. This process was inconsistent and resulted in layers that were thicker at parts than others. This may have resulted in the fabrication of a damper that has different vibration-reducing properties at different cross-sections. Depending on how the device made full contact with the trays, the damper could have performed very differently if adjusted slightly.

A second source of error involves the use of a neonate mannequin during testing that was larger than the average critically-ill neonate which would require transport. Additionally, the mannequin had rigid plastic skin. This may have created excessive vibrations due to the hard plastic bumping against the hard phone. Acquiring a smaller mannequin with skin that better represented the neonate would make the data better reflect the actual neonatal transport experience.

A third source of error is that there were slight deviations from the initial route made during testing. The ambulance experienced speeds of over 70mph on the final test ride but not during baseline testing. This could make comparison of the two data sets erroneous. To make the routes taken as similar as possible, two ambulances could be driven at the same time, one testing the device and one collecting the baseline data. This way, they would experience the same traffic and road conditions. This would ensure that the baseline data could be accurately related to the testing data.

Future Work

Moving forward, the team will work on design optimization and further testing. One potential area for future work related to the prototype is sourcing materials that fit the dimensions of the prototype. For the first iteration of the prototype, layers were cut from material that was larger than the dimensions of the prototype which caused variance in the fit and alignment of the layers within the steel structure. To improve the overall design, performance, and reproducibility of the prototype, materials should be sourced in the dimensions outlined in the design to prevent the need for additional modification.

Another potential area for improvement is the method used for encasing the layers within the steel structure. The current method involves using a spray adhesive to hold the individual layers together and in place, but this can be time-consuming and difficult to achieve consistently. Additionally, the spray adhesive was difficult to use with the silicone gel material and often came apart without any significant force. New methods are currently being explored to increase the efficiency and effectiveness of encasing the layers within the steel structure.

A third area for future work is the identification and use of a computer simulation to test the elastic and damping response of various materials. Our current testing methods involve physical experiments, which can be costly and time-consuming. By using a computer simulation, one could evaluate the performance of different materials under a variety of conditions more efficiently. This could help identify the best materials for use in the design.

Building upon the previous limitations in the current testing set-up, the MATLAB app accelerometer is not ideally suited for the type of testing being conducted, so the use of an alternative accelerometer that will more appropriately collect data in the ambulance setting could increase the accuracy, reliability, and capacity of testing. The implementation of a different accelerometer could assist in evaluating the performance of prototypes and identifying areas for further improvement.

Beyond the modifications and considerations related to the metal and gel composite damper, the team has also evaluated the addition of a head restraint and the incorporation of the shock-absorbing mat into a system that would reduce vibration via a multi-faceted approach. The current standard restraint system in the isolette features a five-point harness with straps across the shoulder, hips, and legs. A study conducted at Carleton University investigated the vibration levels experienced by neonates in the use of the standard harness and a proposed head restraint system [19]. The head restraint system included straps across the forehead and torso with lateral supports on either side of the head. In the study, this system was proven to reduce vibrations experienced by the neonate by 1.7-3.3 times in comparison to the standard system. This set-up could be added as an accessory to future designs to extend reduction of vibration by stabilizing the patient directly. The shock-absorbing mat, as described in the preliminary designs section, would require little modification of the existing system and could reduce the magnitude of the vibrational force experienced by the metal and gel composite damper, increasing effectiveness of the system overall. All three elements could be implemented into the existing transport set-up

with the goal of mitigating vibrational forces through stabilization and diversion of forces applied by the floor during movement.

VIII. Conclusions

Transporting a critically-ill neonate to a Neonatal Intensive Care Unit (NICU) is likely to reduce their chances of survival compared to those that do not require transport. A vibration-reducing device could help increase the neonate's chances of survival. The chosen design of the metal and gel composite damper uses a multilayered material with concentric layers of stainless steel, foam, aluminum, and silicone gel based on the anatomy of a woodpecker's beak. The two L-shaped dampers sit near the neonate's head in between the corners of the inner and outer trays inside the incubator. The two straight side dampers are placed between the trays and along the sides. Due to time constraints, the project's scope focused solely on the vibrational component with mitigating sound as a future objective. Using computerized testing programs such as tensile/compression testing in Solidworks to test different materials for the dampers could help immensely in picking different materials better suited for reducing the vibrations experienced by the neonate. This could include evaluating the effectiveness of porous materials, which have been proven to act as low-pass mechanical filters [20]. In addition to altering the current design, using components of other proposed ideas, like adding foam padding between hard surfaces, could help achieve the team's goal. Using the head and torso restraint could also benefit the neonate in reducing vibrations and adding a sound reduction component.

IX. References

[1] "Transport of the Critically Ill Newborn: Overview, Administrative Aspects of Neonatal Transport Services, Neonatal Team Skills." https://emedicine.medscape.com/article/978606-overview?reg=1 (accessed Oct. 11, 2022).

[2] K. Helenius, N. Longford, L. Lehtonen, N. Modi, and C. Gale, "Association of early postnatal transfer and birth outside a tertiary hospital with mortality and severe brain injury in extremely preterm infants: observational cohort study with propensity score matching," *The BMJ*, vol. 367, p. l5678, Oct. 2019, doi: 10.1136/bmj.l5678.

[3] A. Synnes *et al.*, "Determinants of developmental outcomes in a very preterm Canadian cohort," *Arch. Dis. Child. Fetal Neonatal Ed.*, vol. 102, no. 3, pp. F235–F234, May 2017, doi: 10.1136/archdischild-2016-311228.

[4] American Academy of Pediatrics and American College of Obstetricians and Gynecologists, Eds., *Guidelines for perinatal care*, 7th ed. Elk Grove Village, IL : Washington, DC: American Academy of Pediatrics ; American College of Obstetricians and Gynecologists, 2012.

[5] R. A. Boland, P. G. Davis, J. A. Dawson, and L. W. Doyle, "Outcomes of infants born at 22-27 weeks' gestation in Victoria according to outborn/inborn birth status," *Arch. Dis. Child. Fetal Neonatal Ed.*, vol. 102, no. 2, pp. F153–F161, Mar. 2017, doi: 10.1136/archdischild-2015-310313.

[6] "Preterm birth." https://www.who.int/news-room/fact-sheets/detail/preterm-birth (accessed Oct. 11, 2022).

[7] "Recent trends in hospital use by children in England | Archives of Disease in Childhood." https://adc.bmj.com/content/85/3/203.long (accessed Oct. 11, 2022).

[8] S. Kempley, A. Sinha, and b on, "Census of neonatal transfers in London and the South East of England," *Arch. Dis. Child. Fetal Neonatal Ed.*, vol. 89, no. 6, pp. F521–F526, Nov. 2004, doi: 10.1136/adc.2003.029017.

[9] M. I. Levene, C. L. Fawer, and R. F. Lamont, "Risk factors in the development of intraventricular haemorrhage in the preterm neonate.," *Arch. Dis. Child.*, vol. 57, no. 6, pp. 410–417, Jun. 1982.

[10] K. Derry, "C-06-12-60558 Infant Securement On Neonatal Transport In Transport Incubator," p. 4.

[11] J. Zhou, K. Wang, D. Xu, H. Ouyang, and Y. Fu, "Vibration isolation in neonatal transport by using a quasi-zero-stiffness isolator," *J. Vib. Control*, vol. 24, no. 15, pp. 3278–3291, Aug. 2018, doi: 10.1177/1077546317703866.

[12] M. Bailey-vankuren and A. Shukla, "Isolation device for shock reduction in a neonatal transport apparatus," 20070089236, Apr. 26, 2007 Accessed: Sep. 22, 2022. [Online]. Available: https://www.freepatentsonline.com/y2007/0089236.html

[13] J. Lopes, K. Leuraud, D. Klokov, C. Durand, M.-O. Bernier, and C. Baudin, "Risk of Developing Non-Cancerous Central Nervous System Diseases Due to Ionizing Radiation Exposure during Adulthood: Systematic Review and Meta-Analyses," *Brain Sci.*, vol. 12, no. 8, Art. no. 8, Aug. 2022, doi: 10.3390/brainsci12080984.

[14] P. Ballabh, "Intraventricular Hemorrhage in Premature Infants: Mechanism of Disease," *Pediatr. Res.*, vol. 67, no. 1, pp. 1–8, Jan. 2010, doi: 10.1203/PDR.0b013e3181c1b176.

[15] I. Goswami, "Whole-body vibration in neonatal transport: a review of current knowledge and future research challenges - ClinicalKey." https://www-clinicalkey-com.ezproxy.library.wisc.edu/#!/content/playContent/1-s2.0-S0378378220302139?returnurl=null&referrer=null (accessed Sep. 21, 2022).

[16] "AboutKidsHealth." https://www.aboutkidshealth.ca:443/article?contentid=1810&language=english (accessed Dec. 14, 2022).

[17] "Voyager – int-bio." https://int-bio.com/neonatal-transport/transport-incubators/voyager/ (accessed Oct. 12, 2022).

[18] A. Almadhoob and A. Ohlsson, "Sound reduction management in the neonatal intensive care unit for preterm or very low birth weight infants," *Cochrane Database Syst. Rev.*, vol. 2020, no. 1, p.

CD010333, Jan. 2020, doi: 10.1002/14651858.CD010333.pub3.
[19] B. Biju, A. Ramesh, A. R. Krishnan, A. G. Nath, and C. J. Francis, “Damping characteristics of woodpecker inspired layered shock absorbing structures,” *Mater. Today Proc.*, vol. 25, pp. 140–143, 2020, doi: https://doi.org/10.1016/j.matpr.2019.12.187.
[20] S.-H. Yoon and S. Park, “A mechanical analysis of woodpecker drumming and its application to shock-absorbing systems,” *Bioinspir. Biomim.*, vol. 6, no. 1, p. 016003, Jan. 2011, doi: 10.1088/1748-3182/6/1/016003.
[21] “Properties: Stainless Steel - Grade 304 (UNS S30400),” *AZoM.com*. https://www.azom.com/properties.aspx?ArticleID=965 (accessed Dec. 11, 2022).
[22] “McMaster-Carr.” https://www.mcmaster.com/ (accessed Sep. 30, 2022).
[23] “Seals Eastern 5353 Nitrile Rubber.” https://www.matweb.com/search/datasheet.aspx?matguid=6885f5466aaf4ccd93122b6c25fee040&ckck=1 (accessed Dec. 11, 2022).
[24] A. Elements, “Aluminum Foil,” *American Elements*. https://www.americanelements.com/aluminum-foil-7429-90-5 (accessed Dec. 11, 2022).
[25] I. Rotaru, C. Bujoreanu, A. Bele, M. Cazacu, and D. Olaru, “Experimental testing on free vibration behaviour for silicone rubbers proposed within lumbar disc prosthesis,” *Mater. Sci. Eng. C*, vol. 42, pp. 192–198, Sep. 2014, doi: 10.1016/j.msec.2014.05.021.
[26] “Remove polynomial trend - MATLAB detrend.” https://www.mathworks.com/help/matlab/ref/detrend.html (accessed Dec. 04, 2022).
[27] “What Is the Bonferroni Correction?” https://www.aaos.org/aaosnow/2012/apr/research/research7/ (accessed Dec. 12, 2022).
[28] L. Blaxter *et al.*, “Neonatal head and torso vibration exposure during inter-hospital transfer,” *Proc. Inst. Mech. Eng. [H]*, vol. 231, no. 2, pp. 99–113, Feb. 2017, doi: 10.1177/0954411916680235.
[29] A. Avasthi, A. Ghosh, S. Sarkar, and S. Grover, “Ethics in medical research: General principles with special reference to psychiatry research,” *Indian J. Psychiatry*, vol. 55, no. 1, pp. 86–91, Mar. 2013, doi: 10.4103/0019-5545.105525.
[30] C. for D. and R. Health, “Classify Your Medical Device,” *FDA*, Oct. 22, 2020. https://www.fda.gov/medical-devices/overview-device-regulation/classify-your-medical-device (accessed Sep. 20, 2022).
[31] C. for D. and R. Health, “Sterilization for Medical Devices,” *FDA*, Sep. 2022, Accessed: Sep. 21, 2022. [Online]. Available: https://www.fda.gov/medical-devices/general-hospital-devices-and-supplies/sterilization-medical-devices

X. **Appendix**

Appendix A: Product Design Specifications

Product Design Specifications: Neonatal Transport Unit

September 23, 2022

BME 300/200

Clients: Dr. Ryan McAdams and Dr. Joshua Gollub

Advisor: Dr. Justin WIlliams

Team Members:

Team Leader: Joshua Varghese

Communicator: Sydney Therien

BWIG: Neha Kulkarni

BWIG: Julia Salita

BPAG: Joey Byrne

BSAC: Greta Scheidt

Function:

Critically ill neonates as a result of birth defects or other disorders require transport to neonatal intensive care units (NICU). The quality of that transport heavily influences survival or morbidity [1]. Transport in ambulances or helicopters, while necessary, induces physiological stressors including vibration, translational inertia forces, and rotational inertia moments [2]. These environmental exposures are associated with intraventricular hemorrhage (IVH) in transferred neonates, leading to subsequent neurodevelopmental impairment or death [3]. The current transport incubator has ventilators, monitoring equipment, and temperature control mechanisms, but no control of the physical stressors aforementioned. The natural frequencies of the incubator (12-16 Hz) accentuates the ambulance's natural frequencies (2.5-15 Hz), resulting in amplified vibration felt by the neonate [4]. The proposed device will oppose the mechanical forces transmitted through the transport vehicle or undergo purposeful motion which acts to absorb such forces. The device will improve neonatal transport outcomes by mitigating the effects of vibration and motion, improving the safety of the critical neonate, and simplifying the required care by the medical transport team.

Client Requirements:

1. The device must minimize vibrational forces such that a critical neonate does not sustain injury.
2. The device must minimize translational and rotational forces enough to prevent injury to critical neonates.
3. The device must mitigate sound levels experienced by the neonate in order to eliminate stress and injury (maximum accepted level of 45 dB) [5].
4. The device must either attach to current incubators or include all the associated functions including ventilators, monitoring equipment, and temperature control mechanisms.
5. The device must be small enough to fit within a standard ambulance and allow the movement of the transport team.

Design Requirements:

1. Physical and Operational Characteristics:

a. Performance Requirements:

- The product must decrease the amount of whole-body vibrations to be below 0.87 m/s^2 as recommended by the ACGIH for the exposure of adults [2].
- The product should be capable of reducing the volume of excessive sound levels to be below 45 decibels in order to prevent permanent hearing damage while riding in the transport vehicle [6] .
- The product should allow the infant to maintain proper vital signs in a range appropriate for its size, age, and condition:
    - A heart rate between 100 and 160 beats per minute [7].
    - A respiratory rate between 30 and 60 breaths per minute [7].
    - Blood pressure of no less than 30mmHg systolic [8].
    - An oxygen saturation level between 85 and 95% [9].

b. Safety:

- The transport bed must allow for continuous treatment and should not disrupt the incubator, mechanical ventilator, or monitoring equipment.
- The device should be sterilizable and resistant to degradation that can be caused by common sterilization chemicals such as ethylene oxide [10].
- The device must not have any sharp edges or long cords that the neonate could interact with.

c. Accuracy and Reliability:

- The device should require no maintenance during its lifetime, but should be easy to remove or replace if any malfunctions occur.
- The device should be functional for neonates ranging from 0.66 to 12 pounds [11].

d. Life in Service:

- The service life of a device should allow for 5,000 lifetime transports, or an estimated 5 years of operation, assuming that all ideal practices and operating conditions are followed.

e. Shelf Life:

- The device should last for a minimum of 7 years if any electrical components are involved in the design or a minimum of 12 years if no electrical components are included [12].

f. Operating Environment:

- The operating environment of the device will be ground transport using an ambulance with an incubator [13].

g. Ergonomics:

- The device should have a simple screen interface to control any electrical components.
- The entire device will be designed such that it causes no interference to ambulance personnel when installed and functional.

h. Size:

- The device should be able to fit inside the Voyager transport incubator by International Biomedical, which has dimensions of 53cm H x 48cm W x 99cm L [14].
    - The device could also be created to fit inside the ambulance under the incubator.

i. Weight:

- The device should be no more than 10lb which is equivalent to 5% of the incubator's weight when empty [15].

k. Materials:

- The materials should be safe to use in a medical environment and be in compliance with all federal EMS regulations. [13].

l. Aesthetics, Appearance, and Finish:

- The device should be entirely white or gray to make it easy to identify when cleaning is required [16].

- The device should be distinguishable enough from the incubator that it is not a challenge to locate and remove.
- Aesthetics should not impede the functionality of the device.

2. Product Characteristics:

a. Quantity:

- One functional prototype should be developed by the end of the semester.
- Once refined, the prototype will be mass produced for the general market.

b. Target Product Cost:

- The device will cost no more than $500 to fabricate and test.

3. Miscellaneous:

a. Standards and Specifications :

- The device must be compatible with a sterilization process in accordance with ISO 14937 [17].
- The product will be a Class II medical device according to FDA standards due to moving components that pose some risk to the patient and measurement capabilities [18].
    - FDA approval will be required for commercial use of the device.
- The device must comply with ISO 2631 which sets acceptable frequencies of whole body vibration, established to minimize health risk and discomfort [19].
    - Specifies that for health and comfort, vibrations should not exceed 0.5-80Hz.
    - Specifies that for patients that are motion sick, vibrations should not exceed 0.1-0.5Hz.
- IEC 60601-2-20 sets standards for the basic safety and essential performance of neonatal transport incubators [20]. This standard has been recognized by the FDA under Sec. 880.5410.

b. Customer:

- The target customer for our product is a hospital; specifically, the department within the hospital that manages neonatal transport and/or a Neonatal Intensive Care Unit (NICU).

- The device should be easily compatible with the equipment already used by the hospital, including incubators, transport carts, ambulances, and any accessory equipment used to treat patients during transport.

c. Patient-Related Concerns:

- The device should not pose additional risks to the patient during transport.
- Thorough testing must be completed to ensure the device does not decrease comfortability for the patient.

d. Competition:

- One category of competing designs involves the use of passive vibration isolation systems such as the use of a quasi-zero-stiffness (QZS) isolator placed beneath the infant compartment. This design has a high ability to attenuate low frequency vibrations [21].
- Magnetorheological (MR) dampers address variations in the international roughness index and the curve radius of roads in order to reduce vibrations within the vehicle. The pneumatic suspension system can be toggled between a compliant and stiff setting while the MR damper has an adjustable continuous range of viscosities that allow it to work in tandem with the pneumatic suspensions to reduce vibrations [22].
- A plate mounted to the incubator and another to the stretcher with a gap in between. Between the parallel plates springs are attached, “preferably gas springs, with a range and a damping effect” [23]. The spring reduces vibrations transmitted to the infant during transport.

References:

[1] R. A. Boland, P. G. Davis, J. A. Dawson, and L. W. Doyle, “Outcomes of infants born at 22-27 weeks’ gestation in Victoria according to outborn/inborn birth status,” Arch. Dis. Child. Fetal Neonatal Ed., vol. 102, no. 2, pp. F153–F161, Mar. 2017, doi: 10.1136/archdischild-2015-310313.

[2] I. Goswami, “Whole-body vibration in neonatal transport: a review of current knowledge and future research challenges - ClinicalKey.” July 2020. https://www-clinicalkey-com.ezproxy.library.wisc.edu/#!/content/playContent/1-s2.0-S0378378220302139?returnurl=null&referrer=null (accessed Sep. 21, 2022).

[3] M. I. Levene, C. L. Fawer, and R. F. Lamont, “Risk factors in the development of intraventricular haemorrhage in the preterm neonate.,” Arch. Dis. Child., vol. 57, no. 6, pp. 410–417, Jun. 1982.

[4] G. Gajendragadkar, J. A. Boyd, D. W. Potter, B. G. Mellen, G. D. Hahn, and J. P. Shenai, “Mechanical Vibration in Neonatal Transport: A Randomized Study of Different Mattresses,” J. Perinatol., vol. 20, no. 5, Art. no. 5, Jul. 2000, doi: 10.1038/sj.jp.7200349.

[5] A. Almadhoob and A. Ohlsson, “Sound reduction management in the neonatal intensive care unit for preterm or very low birth weight infants,” Cochrane Database Syst. Rev., vol. 2020, no. 1, p. CD010333, Jan. 2020, doi: 10.1002/14651858.CD010333.pub3.

[6] “What Decibel Level Is Safe for Babies | Safe Noise Levels for Babies,” Decibel Meter App | Best Digital Sound Level Meter For Your Smartphone, Jun. 27, 2021. https://decibelpro.app/blog/safe-decibel-levels-for-babies/ (accessed Sep. 21, 2022).

[7] S. Reuter, C. Moser, and M. Baack, “Respiratory Distress in the Newborn,” Pediatr. Rev., vol. 35, no. 10, pp. 417–429, Oct. 2014.

[8] “Blood pressure disorders | Safer Care Victoria.” https://www.safercare.vic.gov.au/clinical-guidance/neonatal/blood-pressure-disorders (accessed Sep. 23, 2022).

[9] American Academy of Pediatrics and American College of Obstetricians and Gynecologists, Eds., Guidelines for perinatal care, 7th ed. Elk Grove Village, IL : Washington, DC: American Academy of Pediatrics ; American College of Obstetricians and Gynecologists, 2012.

[10] C. for D. and R. Health, “Sterilization for Medical Devices,” FDA, Sep. 2022, Accessed: Sep. 21, 2022. [Online]. Available: https://www.fda.gov/medical-devices/general-hospital-devices-and-supplies/sterilization-medical-devices

[11] “Baby weight chart: what’s the average weight for a newborn? | GoodTo.” https://www.goodto.com/family/babies/your-baby-s-weight-69876 (accessed Sep. 21, 2022).

[12] S. Loznen, “Expected Service Life of Medical Electrical Equipment,” In Compliance Magazine. https://incompliancemag.com/article/expected-service-life-of-medical-electrical-equipment/ (accessed Sep. 21, 2022).

[13] H. H. de Anda and H. P. Moy, “EMS Ground Transport Safety,” in StatPearls, Treasure Island (FL): StatPearls Publishing, 2022. Accessed: Sep. 22, 2022. [Online]. Available: http://www.ncbi.nlm.nih.gov/books/NBK558971/
[14] “Voyager-DOM-Spec-Sheet-web.pdf.” Accessed: Sep. 23, 2022. [Online]. Available: https://int-bio.com/wp-content/uploads/2022/03/Voyager-DOM-Spec-Sheet-web.pdf
[15] kgrant, “GE Airborne 750i Infant Incubator - Seattle Technology: Surgical Division.” https://stsurg.com/product/ge-airborne-750i-infant-incubator/ (accessed Sep. 21, 2022).
[16] D. Stipe, “Color in Medical Products.” https://formamedicaldevicedesign.com/white-papers/color-medical-products/undefined (accessed Sep. 23, 2022).
[17] “ISO 14937:2009(en), Sterilization of health care products — General requirements for characterization of a sterilizing agent and the development, validation and routine control of a sterilization process for medical devices.” https://www.iso.org/obp/ui/#iso:std:iso:14937:ed-2:v1:en (accessed Sep. 21, 2022).
[18] C. for D. and R. Health, “Classify Your Medical Device,” FDA, Oct. 22, 2020. https://www.fda.gov/medical-devices/overview-device-regulation/classify-your-medical-device (accessed Sep. 20, 2022).
[19] “ISO 2631-1:1997(en), Mechanical vibration and shock — Evaluation of human exposure to whole-body vibration — Part 1: General requirements.” https://www.iso.org/obp/ui/#iso:std:iso:2631:-1:ed-2:v2:en (accessed Sep. 18, 2022).
[20] “IEC 60601-2-20:2020 RLV | IEC Webstore.” https://webstore.iec.ch/publication/67567 (accessed Sep. 21, 2022).
[21] J. Zhou, K. Wang, D. Xu, H. Ouyang, and Y. Fu, “Vibration isolation in neonatal transport by using a quasi-zero-stiffness isolator,” J. Vib. Control, vol. 24, no. 15, pp. 3278–3291, Aug. 2018, doi: 10.1177/1077546317703866.
[22] A. L. Morales, A. J. Nieto, J. M. Chicharro, and P. Pintado, “A semi-active vehicle suspension based on pneumatic springs and magnetorheological dampers,” J. Vib. Control, vol. 24, Jun. 2016, doi: 10.1177/1077546316653004.
[23] M. Bailey-vankuren and A. Shukla, “Isolation device for shock reduction in a neonatal transport apparatus,” 20070089236, Apr. 26, 2007 Accessed: Sep. 22, 2022. [Online]. Available: https://www.freepatentsonline.com/y2007/0089236.html

Appendix B: Materials and Costs

Item	Description	Manufacturer	Part Number	Date	QTY	Cost Each	Total	Link
Component 1: Dampers								
Stainless Steel Rectangular Tube	To be used as the outer housing for the dampers.	Grainger	786G80		1	$22.80	$22.80	Stainless Steel Rectangular Tube
Stainless Steel Sheet	"Caps" that will be welded to the open ends of the rectangular tube	Grainger	796XW3		1	$64.99	$64.99	Stainless Steel Sheet
Vibration-Dampening Pad	Component of the damper inside the rectangular tube	McMaster-Carr	5940K57		1	$51.24	$51.24	Vibration-Damping Pad
Reynolds Wrap Aluminum Foil	Component of the damper inside the rectangular tube	Reynolds (from Target)	N/A		1	$6.29	$6.29	Aluminum Foil
Matte Non-Reinforced Silicone Sheeting	Component of damper inside the rectangular tube	Specialty ManufacturingInc. (SMI)	N/A		1	$26.00	$26.00	Silicone Sheeting
Component 2: Attached Roller								
Stainless Steel Coiled Spring Pin	Attached between the cap nut and damper to reduce vibrational forces	Grainger	41LZ72		1	$22.32	$22.32	Spring Pin
Cap Nut	Attached the cap nut and butting against the incubator tray to allow movement.	Grainger	6NY12		1	$14.64	$14.64	Cap Nut
Component 3: Adhesive								
3M Series 27 Spray Adhesive	Used to attach various components together	3M (from Grainger)	6KWY1		1	$13.68	$13.68	Spray Adhesive
						TOTAL:	**$221.96**	

Appendix C: Fabrication Protocol

Side dampers (x2):

1. Measure and cut the stainless steel tube to 8.25 in long using a drop saw.
2. Square ends using a mill.
3. Use a mill to remove one side by milling down the thickness of the wall (0.065 inches) using a ⅝" colette and end mill.
    a. To do this, place the tube in a vise on parallels with the face you are removing sticking out of the vise just enough that the end mill doesn't hit the vise.
    b. Run the mill at an RPM of 153 and complete two passes, taking off 0.03" each time.
4. After removing one side, shorten one of the exposed remaining walls by 0.09 inches. Creating a slanted edge will allow the damper to sit flush with the outside of the inner tray in the isolette.
5. Cut foam to 8.25 x 0.375 x 0.0625 inch pieces. Cut length and width using a breaker and cut thickness using an X-acto knife.
6. Cut gel to 8.25 x 0.375 x 0.06 inch pieces using scissors.
7. Cut foil to 8.25 x 0.375 inch pieces using scissors.
8. Spray tube with adhesive and place foam piece in bottom of tube. Apply even pressure on the layer for 10-15 seconds.
9. Spray foam with adhesive and place an aluminum foil piece on top. Apply even pressure on the layer for 10-15 seconds.
10. Spray foil with adhesive and place a gel piece on top. Apply even pressure on the layer for 10-15 seconds.
11. Spray gel with adhesive and place additional foil layer on top. Apply even pressure on the layer for 10-15 seconds.
12. Repeat steps 6-8 three times or until a silicone gel layer is flush with the top of the tube.
13. Tinsnip any overhanging edges.
14. Cover the exposed edge with aluminum foil to seal layers.

Corner dampers (x2):

1. Measure and cut the stainless steel sheet to 3.4 in long using a water jet.
2. Bend sheet in the center and to create a bottom edge using a sheet metal bending break.
3. Cut foam to 1.2 x 0.375 x 0.0625 inch pieces using a breaker and an X-acto knife.
4. Cut gel to 1.2 x 0.375 x 0.06 inch pieces using scissors.
5. Cut foil to 1.2 x 0.375 inch pieces using scissors.
6. Spray housing with adhesive and place foam against the side of the stainless steel housing. Apply even pressure on the layer for 10-15 seconds.
7. Spray foam with adhesive and place aluminum foil on top. Apply even pressure on the layer for 10-15 seconds.

8. Spray foil with adhesive and place a gel piece on top. Apply even pressure on the layer for 10-15 seconds.
9. Spray gel with adhesive and place additional foil layer on top. Apply even pressure on the layer for 10-15 seconds.
10. Repeat steps 6-8 three times or until a silicon gel layer is flush with the bottom edge of the stainless steel housing.
11. Tinsip any overhanging edges.
12. Cover any exposed edges with aluminum foil to seal layers.

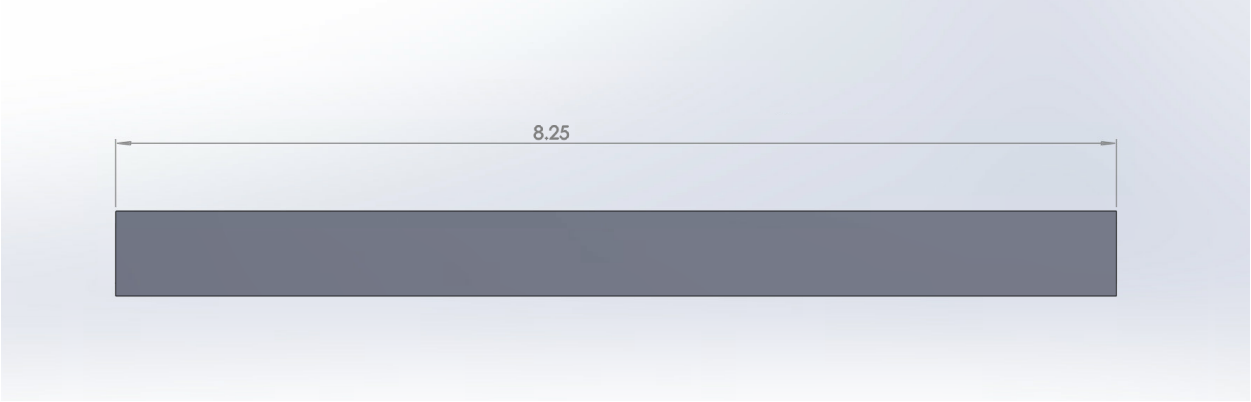

Figure 1: Dimensioned side view of steel housing for straight damper

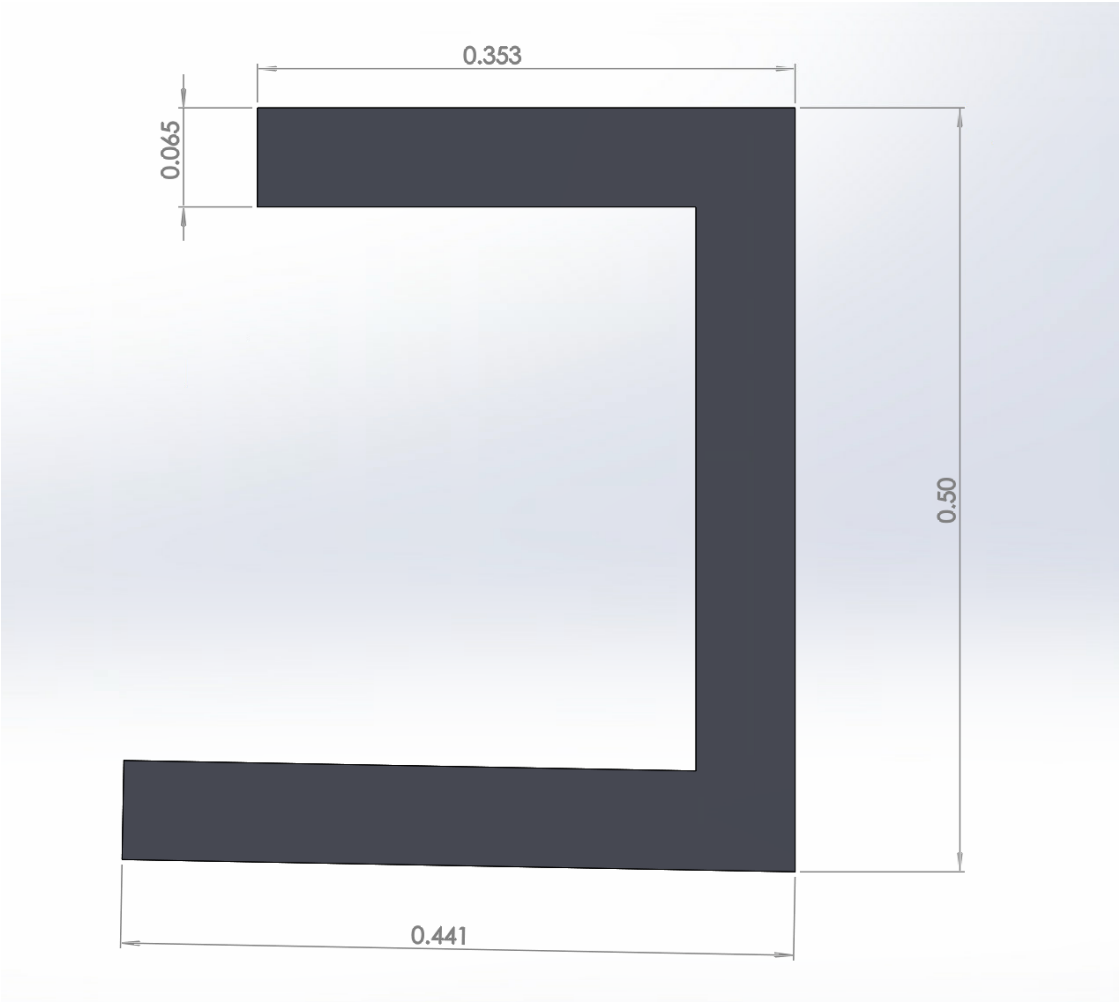

Figure 2: Dimensioned front view of steel housing for side damper.

Appendix D: Raw Data and MATLAB Code

The data and code was too large to fit into this document. The files have been added to a shared Google drive folder which can be accessed via this link: https://drive.google.com/drive/folders/1fRKeyVhMW-5RvR1a_Os-M3_Te2HaVRq9?usp=sharing

Appendix E: Table of P-values

BF-Chest	BF-FF	BF-MS	BF-Head	BF-BS	Chest-FF	Chest-MS	Chest-Head	Chest-BS	FF-MS	FF-Head	FF-BS	MS-Head	MS-BS	Head-BS
2.11E-06	0.01649916164	0.2297876828	5.08E-11	0.1188813254	1.98E-09	7.36E-08	0.5738887063	0.0001149677142	0.2258102827	4.51E-16	9.70E-05	1.77E-13	0.006156338751	4.81E-08
2.89E-52	1.03E-33	5.69E-29	0.00E-01	1.51E-13	5.48E-150	1.38E-145	8.12E-149	7.34E-16	0.1093773871	0	7.11E-81	0	9.39E-76	2.00E-233
9.73E-27	5.93E-91	1.61E-62	2.13E-112	1.28E-11	6.01E-30	4.11E-12	5.95E-232	5.05E-05	1.84E-06	0	4.17E-49	3.86E-302	1.76E-26	9.29E-185
0.9725783185	1.41E-107	2.53E-28	4.18E-200	2.70E-05	1.98E-120	2.36E-31	7.23E-211	1.13E-05	6.13E-38	0	1.12E-87	0	6.65E-14	4.13E-260
2.06E-43	5.06E-68	1.11E-23	0.00E-01	0.5526759336	2.63E-201	2.70E-126	1.44E-176	4.56E-41	7.50E-18	0	5.14E-75	0	2.30E-27	0.00E-01
4.07E-174	7.75E-59	6.91E-11	1.71E-285	1.40E-51	0	2.96E-131	1.50E-42	1.47E-48	3.67E-134	0	1.18E-194	1.60E-244	6.53E-24	1.21E-147
2.36E-76	3.37E-92	0.007359319364	0	3.34E-65	3.00E-288	7.48E-106	1.15E-162	0.1328061537	3.56E-87	0	2.00E-269	0	2.15E-92	3.77E-176
1.61E-103	2.65E-87	0.001164597353	0	2.16E-139	0	8.60E-81	7.82E-114	2.50E-06	5.89E-122	0	0	0.00E-01	6.11E-115	1.08E-73
5.61E-130	1.03E-91	3.00E-23	0	6.71E-183	0	2.13E-51	2.27E-101	3.23E-11	1.08E-183	0	0	1.81E-259	1.20E-94	1.44E-47
7.49E-145	8.77E-76	3.62E-38	5.50E-272	1.81E-151	0	5.64E-51	1.05E-24	0.8917547809	3.06E-205	0	0	9.42E-143	1.30E-53	1.18E-24
3.54E-175	5.11E-57	1.65E-54	0.00E-01	1.60E-157	0	6.12E-51	1.93E-27	0.002680083773	3.72E-194	0	0	4.86E-145	3.40E-36	4.71E-45
1.04E-203	2.22E-48	5.26E-91	0	1.42E-257	0	6.07E-39	2.39E-60	7.53E-08	7.25E-216	0	0	2.26E-171	2.63E-73	1.69E-29
1.81E-170	3.10E-45	4.77E-09	0	1.97E-104	0.00E-01	2.95E-122	2.31E-107	2.21E-16	1.11E-88	0	1.79E-245	0	1.20E-62	3.01E-188
6.67E-183	2.48E-18	0.3488543683	0	5.71E-10	2.46E-264	5.36E-177	1.92E-76	2.12E-131	1.05E-22	0	6.04E-50	0	8.92E-08	0
1.19E-234	0.2211626602	0.1491917286	0	4.97E-05	7.22E-250	2.84E-225	1.36E-87	2.23E-199	0.006541919358	0	8.15E-08	0	0.007268700079	0
9.41E-277	0.5555708249	0.1503985362	0	0.510725727	1.76E-280	3.11E-295	2.08E-82	5.33E-291	0.03459199659	0	0.1915591474	0	0.4095746343	0
0	0.005679731292	0.03522568065	0	0.9953196742	0	0	2.18E-95	0	4.85E-07	0	0.005631587828	0	0.03597268181	0
0	2.14E-08	0.05503694239	0	2.24E-15	0	0	2.17E-108	0.00E-01	0.0001205558151	0	0.003562715337	0	1.51E-10	0
0	5.56E-06	1.88E-12	0	1.92E-83	0	0	6.67E-61	1.47E-277	0.01541916897	0	2.30E-54	0	1.85E-42	0
0	1.28E-17	6.80E-29	0	1.84E-200	0	0	6.55E-45	2.83E-251	0.008762271123	0	1.96E-125	0	2.43E-105	0
0	7.80E-10	0.003277568681	0	3.74E-130	0	0	1.46E-57	4.78E-199	0.0007860212602	0	5.34E-78	0	1.80E-107	0
8.16E-299	9.00E-14	0.1326703134	0	6.27E-52	2.58E-239	2.79E-295	6.72E-111	2.54E-168	2.78E-10	0	1.53E-16	0	4.88E-47	0
6.85E-170	1.68E-24	0.117208316	0	9.66E-09	1.32E-77	2.06E-184	9.23E-229	2.53E-101	1.89E-31	0	0.0001424528552	0	1.12E-12	0
2.15E-64	1.34E-18	4.95E-19	0	2.47E-11	5.06E-17	6.07E-130	0.00E-01	2.62E-105	6.25E-64	0	2.15E-47	0	0.1058377924	0

1.69E-99	2.17E-14	6.48E-44	0	1.33E-21	2.37E-46	1.05E-225	4.21E-304	4.29E-176	4.41E-96	0	6.49E-61	0	0.0001902257271	0
1.79E-101	2.89E-13	2.81E-21	0	5.11E-10	2.02E-49	2.78E-179	0	4.56E-147	2.06E-58	0	2.36E-38	0	0.002657861696	0
2.57E-96	1.23E-05	3.84E-19	0	6.35E-09	5.66E-64	8.37E-168	0	4.15E-139	3.27E-38	0	4.79E-23	0	0.002505546885	0
1.27E-105	0.0287530 1655	2.47E-12	0	5.18E-10	6.20E-89	2.05E-165	0	8.79E-159	5.49E-20	0	5.38E-17	0	0.4048612029	0
2.37E-92	0.0004399803001	1.05E-09	0	2.31E-15	2.17E-125	6.46E-152	0	5.71E-168	0.008992598611	0	5.41E-06	0	0.04341514119	0
5.98E-115	0.0786496 1418	0.0173663 5743	0	1.58E-13	1.89E-131	3.53E-142	0	1.34E-194	0.5682717655	0	2.27E-08	0	2.04E-07	0
2.12E-120	0.5909258232	0.7739569263	0	1.03E-20	3.92E-119	2.81E-126	1.98E-307	4.20E-230	0.3998753198	0	3.19E-24	0	2.12E-20	0
9.85E-120	0.6176979978	0.0317122 0448	0	2.70E-57	4.72E-127	3.64E-143	3.53E-274	0.00E-01	0.0936016934	0	3.64E-56	0	1.71E-45	0
1.23E-96	0.7051410 54	2.07E-23	0	1.51E-98	3.44E-97	9.80E-197	1.21E-289	0	7.35E-21	0	2.01E-90	0	4.13E-32	0
2.95E-99	0.5000530962	5.62E-47	0	4.66E-117	1.22E-93	1.84E-256	3.65E-301	0	2.59E-51	0	1.32E-123	0	1.49E-21	0
5.60E-88	0.0572323 1579	2.26E-61	0	2.72E-114	7.03E-72	8.37E-282	0	0	1.08E-74	0	6.58E-131	0	1.23E-12	0
2.94E-86	7.95E-06	9.15E-85	0	2.05E-146	5.14E-51	0.00E-01	0	0	2.28E-119	0	8.91E-186	0	6.73E-13	0
2.12E-82	6.14E-08	3.34E-73	0	2.87E-152	1.75E-42	1.28E-291	0	0	5.31E-117	0	2.32E-206	0	6.04E-22	0
1.29E-63	6.34E-10	5.07E-90	0	2.24E-142	2.37E-23	2.01E-280	0	0	5.41E-134	0	1.42E-188	0	8.24E-09	0
1.03E-45	4.49E-26	4.72E-66	0	2.71E-123	0.0070457 7679	2.04E-215	0	6.82E-306	2.37E-151	0	6.80E-221	0	3.66E-13	0
3.42E-06	6.60E-20	1.95E-42	0	2.45E-133	7.29E-08	1.03E-82	0	5.14E-217	2.34E-102	0	1.92E-212	0	8.80E-27	0
0.006569672408	1.04E-33	5.80E-20	0	7.23E-105	2.87E-52	3.47E-13	0	6.37E-102	4.36E-89	6.83E-269	3.03E-214	0	1.02E-30	0
5.05E-27	1.26E-19	8.10E-09	0	3.44E-137	1.81E-81	0.0005108022537	0	3.94E-68	5.15E-43	1.66E-269	4.80E-210	0	4.34E-61	0
1.30E-53	4.06E-22	1.13E-14	1.41E-298	7.76E-165	2.57E-125	3.17E-09	0	8.07E-49	3.89E-59	8.30E-225	5.64E-251	0	1.03E-65	0
1.63E-94	1.57E-15	1.93E-45	0.00E-01	1.80E-159	3.04E-155	2.31E-07	0	3.69E-17	7.95E-95	1.07E-220	4.83E-222	0	1.71E-33	0
2.59E-157	2.22E-14	2.34E-93	1.82E-273	6.41E-170	1.97E-218	1.09E-09	0	0.06035693872	9.07E-151	3.77E-180	8.37E-231	0	1.88E-14	0
1.14E-200	8.09E-10	4.15E-115	2.53E-241	1.05E-185	1.52E-241	8.87E-19	0	0.2283181596	1.69E-158	1.71E-165	1.32E-227	0	4.28E-14	0
4.44E-248	4.13E-05	7.90E-142	1.79E-193	1.23E-219	2.95E-285	1.81E-25	0	0.01324069499	1.32E-177	1.26E-146	5.22E-257	0	2.79E-15	0
1.32E-279	8.52E-06	1.99E-156	3.38E-166	3.27E-227	0.00E-01	1.23E-34	0	2.52E-07	4.97E-192	2.03E-118	5.87E-262	0	4.25E-13	0
1.11E-302	0.3200484159	1.65E-173	2.46E-153	2.34E-222	0	9.14E-39	0	6.98E-17	1.69E-189	1.53E-145	7.22E-241	0	6.99E-07	0
6.33E-275	0.0001111712828	8.55E-153	7.47E-157	2.90E-211	8.12E-296	2.38E-32	0	1.19E-10	2.05E-179	3.35E-114	5.29E-236	0	1.18E-08	0

Chest_Orig-Chest	Head_Orig-Head	Chest_Orig-Head	Head_Orig-Chest

4.86E-30	1.47E-51	1.67E-51	4.49E-30
5.30E-188	1.08E-20	7.94E-33	2.18E-157
3.18E-23	6.09E-93	4.48E-86	1.02E-17
0.07336942858	9.24E-168	1.28E-173	1.87E-01
3.42E-08	1.61E-71	2.33E-85	6.81E-12
2.75E-126	6.97E-61	2.21E-29	1.22E-168
0	3.71E-261	5.63E-240	0.00E+00
1.33E-283	5.58E-218	9.42E-118	0
1.06E-39	0.1371537404	2.46E-05	2.72E-72
1.42E-42	0.8715543209	3.61E-10	2.75E-15
1.30E-64	1.41E-07	1.32E-20	1.54E-39
4.19E-73	1.07E-40	4.22E-08	2.83E-129
1.18E-25	3.64E-20	2.39E-18	7.53E-133
0.01123390507	7.73E-19	3.31E-44	4.08E-113
0.1378714458	2.02E-15	6.67E-55	1.51E-117
3.61E-15	6.35E-43	6.51E-18	2.19E-159
1.30E-47	1.02E-101	0.01476654044	1.01E-234
3.48E-31	2.93E-123	4.32E-14	2.22E-284
3.77E-16	2.60E-19	1.16E-102	6.61E-103
8.80E-115	2.36E-68	3.24E-255	4.25E-07
1.55E-90	3.69E-197	3.79E-240	2.57E-60
2.29E-36	2.58E-217	2.17E-182	4.79E-62
0.002240121044	1.69E-202	4.61E-137	2.47E-05
2.76E-06	1.54E-216	1.39E-172	9.02E-01
8.71E-06	0.00E-01	9.19E-263	1.66E-20
2.59E-18	0.00E+00	0.00E-01	7.22E-37
3.41E-17	0.00E+00	0	1.65E-50
1.21E-10	0.00E+00	0.00E-01	6.50E-55
1.87E-22	0	0	1.19E-56
3.00E-20	8.64E-294	0	4.88E-08
1.92E-55	8.88E-117	0	4.53E-24
2.20E-175	4.11E-78	0	1.88E-40
1.40E-260	6.20E-91	0	1.30E-41
0.00E-01	4.67E-111	0	1.03E-32
0	2.22E-167	0	1.24E-20
0	1.17E-187	0	2.06E-19
1.54E-269	3.35E-220	0	2.38E-13
1.50E-186	9.03E-193	0	1.46E-30
3.24E-270	1.44E-250	0	1.27E-10

8.82E-295	0.00E+00	0	5.88E-01
3.38E-301	3.12E-260	0	2.65E-03
1.18E-239	0.00E+00	0	1.14E-15
6.20E-225	0.00E+00	0	2.21E-21
3.00E-209	0.00E+00	0	5.71E-25
1.37E-155	0.00E+00	0	2.65E-16
1.17E-159	0.00E+00	0	3.38E-15
2.03E-144	0.00E+00	0	4.25E-14
1.51E-132	0.00E+00	0	3.02E-13
1.12E-118	0.00E+00	0	2.57E-11
7.61E-105	0.00E+00	0	5.25E-21

Appendix F: Average Acceleration Values

Back Floor	Chest	Front Floor	Middle Sled	Head	Back Sled
0.8776 m/s^2	2.4710 m/s^2	0.8336 m/s^2	0.8372 m/s^2	1.9097 m/s^2	0.9654 m/s^2